PHYSICAL REVIEW D **78,** 085008 (2008)

One-loop corrections to the string tension of the vortex in the Abelian Higgs model

Jurgen Baacke*
Fachbereich Physik, Technische Universität Dortmund. D–44221 Dortmund, Germany

Nina Kevlishvili+
Dipartimento di Fisica, Universita degli studi di Ferrara, I-44100 Ferrara, Italy,
INFN, Sezione di Ferrara, I-44100 Ferrara, Italy,
and Andronikashvili Institute of Physics, GAS, 0177 Tbilisi, Georgia
(Received 3 July 2008; published 13 October 2008)

We present an exact numerical computation of the one-loop correction of the string tension for the Nielsen-Olesen vortex in the Abelian Higgs model. The computation proceeds via the computation of the Euclidean Green's function for the gauge, Higgs, and Faddeev-Popov fields using mode functions, and taking the appropriate trace. Renormalization is an essential part of this computation. It is done by removing leading order contributions from the numerical results so as to make these finite, and to add the divergent parts back, after suitable regularization and renormalization. We encounter and solve some problems which are specific to gauge theories and topological solutions. The corrections to the energy are found to be sizable, but still smaller than the classical energy as long as g^2 is smaller than unity.

DOI: 10.1103/PhysRevD.78.085008 PACS numbers: 11.15.Kc, 11.27.+d, 98.80.Cq

I. INTRODUCTION

Extended classical solutions that can be interpreted as strings exist in various realistic and semirealistic models of particle physics [1,2]. Their possible role in cosmology has been evocated long ago [3], see [4,5] for reviews. In confrontation with the recent wealth of cosmological observations they present a very interesting and active, but still controversial, field of research, see e.g. [6,7].

In the present investigation we consider the string that is made up by the vortex solution of the Abelian Higgs model in $3+1$ dimensions, well known from superconductivity [8], and commonly denoted in particle physics as the Nielsen-Olesen vortex [9]. The $1+1$ dimensional version of this solution represents an instanton solution that has been widely considered in the context of baryon number violation.

There have been various investigations of the one-loop correction to the string tension. The fermionic corrections to the energy of the Nielsen-Olesen vortex have been computed exactly in Ref. [10]. Fermionic corrections to strings in $2+1$ and $3+1$ dimensions have also been considered by various other authors [11–14]. Such calculations may be important in the context of the instability of the electroweak string [15].

Here we consider the energy corrections arising from the gauge-Higgs and Faddeev-Popov sector. There are some previous investigations, using heat kernel techniques [16,17]. Here we attempt an exact computation, using techniques that have been developed previously in Refs. [18–21] and applied in various semiclassical computations, of one-loop energy corrections and one-loop prefactors to transition rates. The computations have three essential ingredients: the use of mode functions (''Jost functions,'' see e.g., [22]) in order to compute exact results, the use of perturbative subtractions, so as to make these results finite, and the computation of the subtracted parts using a covariant regularization and renormalization scheme. Similar approaches have been used recently by other authors, see e.g. [23–26]. In a gauge theory as considered here, one finds some complications due to the fact that there are cancellations of divergences between graphs of a different number of vertices. This will be discussed in detail in the context of renormalization.

Whether the energy corrections are small or big depends, in the present case, on the gauge coupling. The classical string tension is proportional to $v^2 = m_W^2/g^2$, where g is the gauge coupling, while the corrections are proportional to m_W^2 multiplied by a function of $\xi = m_H/m_W$. So the corrections are necessarily small relative to the classical string tension if g is sufficiently small. If ever the corrections are big, then this signals the breakdown of the semiclassical method. In intermediate situations one may have recourse to a Hartree-type approximation by including the backreaction of the quantum fluctuations to the classical solution. The methods we use here are suitable for such investigations [27,28], or even for self-consistent calculations without a classical solution [29].

The text is organized as follows: In Sec, II we present the model, the classical vortex solution, and the classical string tension. In Sec, III we relate in general the fluctuation operator to the one-loop correction to the string tension, and we explicitly derive the fluctuation operator. Its partial wave reduction is presented in Sec. IV. This is the basis for

*juergen.baacke@tu-dortmund.de
+nkevli@fe.infn.it

the actual numerical computation of the one-loop string tension, which is described in Sec. V. Renormalization is discussed in some detail in Sec. VI. In Sec. VII we give some details of the numerical implementation and present the results. We conclude with a summary in Sec. VIII. Some technical details are discussed in Appendices A, B, C, D, E, F, and G.

II. BASIC RELATIONS

The Abelian Higgs model in $(3+1)$ dimensions is defined by the Lagrange density

$$\mathcal{L} = -\frac{1}{4}F_{\mu\nu}F^{\mu\nu} + \frac{1}{2}(D_\mu\phi)^* D^\mu\phi - \frac{\lambda}{4}(|\phi|^2 - v^2)^2. \tag{2.1}$$

Here ϕ is a complex scalar field and

$$F_{\mu\nu} = \partial_\mu A_\nu - \partial_\nu A_\mu, \tag{2.2}$$

$$D_\mu = \partial_\mu - igA_\mu. \tag{2.3}$$

The particle spectrum consists of Higgs bosons of mass $m_H^2 = 2\lambda v^2$ and vector bosons of mass $m_W^2 = g^2 v^2$. The model allows for vortex-type solutions, representing strings with a magnetic flux, the Nielsen-Olesen vortices [8,9,30,31]. The cylindrically symmetric ansatz for this solution is given by [32]

$$A_i^{\mathrm{cl},\perp}(x,y,z) = \frac{\epsilon_{ij}x_j^\perp}{gr^2}A(r) i = 1,2, \tag{2.4}$$

$$\phi^{\mathrm{cl}}(x,y,z) = vf(r)e^{i\varphi(x)}, \tag{2.5}$$

where $r = \sqrt{x^2+y^2}$ and φ is the polar angle. Furthermore $A_3^{\mathrm{cl}} = A_0^{\mathrm{cl}} = 0$. In order to have a purely real Higgs field, one performs a gauge transformation

$$\phi \to e^{-i\varphi}\phi, \tag{2.6}$$

$$A_i^\perp \to A_i^\perp - \nabla_i^\perp\varphi/g \tag{2.7}$$

to obtain the instanton fields in the singular gauge

$$A_i^{\mathrm{cl}\perp}(x,y,z) = \frac{\epsilon_{ij}x_j^\perp}{gr^2}[A(r)+1] \qquad i = 1,2 \tag{2.8}$$

$$\phi^{\mathrm{cl}}(x,y,z) = vf(r). \tag{2.9}$$

With this ansatz the energy per unit length, or string tension σ, takes the form

$$\sigma_{\mathrm{cl}} = \pi v^2 \int_0^\infty dr\Big\{\frac{1}{rm_W^2}\Big[\frac{dA(r)}{dr}\Big]^2 + r\Big[\frac{df(r)}{dr}\Big]^2 + \frac{f^2(r)}{r}[A(r)+1]^2 + \frac{rm_H^2}{4}[f^2(r)-1]^2\Big\}. \tag{2.10}$$

The magnetic flux is given by

$$\Phi_M = \int d^2x B_3 = -\int dxdy F_{12}. \tag{2.11}$$

Explicitly we find

$$\Phi_M = \int d^2x(\nabla_1^\perp A_2^{\mathrm{cl}\perp} - \nabla_2^\perp A_1^{\mathrm{cl}\perp}) = \int d\phi r dr\Big[\frac{-1}{gr}A'(r)\Big] = \frac{2\pi}{g}[A(0) - A(\infty)]. \tag{2.12}$$

For the case $m_H = m_W$ an exact solution to the variational equation is known [30], for which the classical string tension takes the value $\sigma_{\mathrm{cl}} = \pi v^2$. We here will consider the general case $m_W \neq m_H$, for which the classical equations of motion

$$\Big\{\frac{\partial^2}{\partial r^2} + \frac{1}{r}\frac{\partial}{\partial r} - \frac{[A(r)+1]^2}{r^2} - \frac{m_H^2}{2}[f^2(r)-1]\Big\}f(r) = 0, \tag{2.13}$$

$$\Big\{\frac{\partial^2}{\partial r^2} - \frac{1}{r}\frac{\partial}{\partial r} - m_W^2 f^2(r)\Big\}[A(r)+1] = 0 \tag{2.14}$$

have to be solved numerically.

Imposing the boundary conditions on the profile functions

$$A(r) \overset{r\to 0}{\to} \mathrm{const}\cdot r^2, \qquad A(r) \overset{r\to\infty}{\to} -1, \qquad f(r) \overset{r\to 0}{\to} \mathrm{const}\cdot r, \qquad f(r) \overset{r\to\infty}{\to} 1, \tag{2.15}$$

the magnetic flux is $\Phi_M = 2\pi/g$, the Dirac magnetic flux quantum, and the action is finite.

Since we have to consider fluctuations around these solutions, a good numerical accuracy for the profile functions $f(r)$ and $A(r)$ is required. As in previous publications [33,34] we have the method of Bais and Primack [35].

III. FLUCTUATION OPERATOR AND ONE-LOOP STRING TENSION

The fluctuation operator is defined in general form as

$$\mathcal{M} = \frac{\delta^2 S}{\delta\psi_i^*(x)\delta\psi_j(x')}\Big|_{\psi_k=\psi_k^{\mathrm{cl}}}, \tag{3.1}$$

where ψ_i denotes the fluctuating fields and ψ_i^{cl} the "classical" background field configuration; here these will be the vortex and the vacuum configurations. If the fields are expanded around the background configuration as $\psi_i = \psi_i^{\mathrm{cl}} + \phi_i$ and if the Lagrange density is expanded accordingly, then the fluctuation operator is related to the second-order Lagrange density via

$$\mathcal{L}^{II} = \tfrac{1}{2}\phi_i^* \mathcal{M}_{ij}\phi_j. \tag{3.2}$$

In terms of the fluctuation operators $\mathcal{M}$ on the vortex and $\mathcal{M}^0$ on the vacuum backgrounds, the effective action is defined as

$$S_{\text{eff}} = \frac{i}{2}\ln\left\{\frac{\det\mathcal{M} + i\epsilon}{\det\mathcal{M}^0 + i\epsilon}\right\}. \tag{3.3}$$

As the background field is time independent and also independent of z, the fluctuation operators take the form

$$\mathcal{M} = \partial_0^2 - \partial_3^2 + \mathcal{M}_\perp, \tag{3.4}$$

where $\mathcal{M}_\perp$ is a positive-definite operator describing the transversal fluctuations. As is well known the logarithm of the determinant can be written as the trace of the logarithm. One can do the trace over p_0, the momentum associated with the time variable, by integrating over $T\int dp_0/2\pi$, where T is the lapse of time. One then obtains

$$S_{\text{eff}} = -iT\frac{1}{2}\sum[E_\alpha - E_\alpha^{(0)}], \tag{3.5}$$

where E_α are square roots of the eigenvalues of the positive-definite operator

$$-\partial_3^2 + \mathcal{M}_\perp, \tag{3.6}$$

and likewise $E_\alpha^{(0)}$ are those of the analogous operator in the vacuum

$$-\partial_3^2 + \mathcal{M}^0 = -\partial_3^2 - \vec{\nabla}_\perp^2 + \mathbf{m}^2. \tag{3.7}$$

Here $\mathbf{m}^2 = \text{diag}(m_1^2, \ldots, m_n^2)$ is the diagonal mass squared operator for the various fluctuations.

So the effective action becomes equal to the difference between the zero point energies of the fluctuations around the vortex and in the vacuum, multiplied by $-T$. We can also do the trace over the variable p_3 by integration over $L\int dp_3/2\pi$. We then obtain

$$S_{\text{eff}} = -iTL\sum_\alpha \int \frac{dk_3}{2\pi}\frac{1}{2}[\sqrt{k_3^2 + \mu_\alpha^2} - \sqrt{k_3^2 + \mu_\alpha^{(0)\,2}}], \tag{3.8}$$

where μ_α^2 are the eigenvalues of the operator $\mathcal{M}^\perp$ and $\mu_\alpha^{(0)\,2}$ those of $-\vec{\nabla}_\perp^2 + \mathbf{m}^2$. In the same way the classical action becomes

$$S_{\text{cl}} = -TL\sigma_{\text{cl}}, \tag{3.9}$$

where σ_{cl} is the classical string tension. So our goal reduces to computing the one-loop approximation to the string tension given by

$$\sigma_{\text{1-loop}} = \sigma_{\text{cl}} + \sigma_{\text{fl}}, \tag{3.10}$$

where the fluctuation part of the string tension is given by

$$\sigma_{\text{fl}} = \sum_\alpha \int \frac{dk_3}{2\pi}\frac{1}{2}[\sqrt{k_3^2 + \mu_\alpha^2} - \sqrt{k_3^2 + \mu_\alpha^{(0)\,2}}]. \tag{3.11}$$

Of course all expressions are formal, the integrals do not exist before a suitable regularization. Anyway we do not plan to compute any eigenvalues of the fluctuation operators but will reduce these expressions to traces over Euclidean Green's functions, where renormalization will be done properly. However, the formal identities will allow us to trace the way in which the counterterms in the original Lagrangian enter the final expressions that are going to be computed numerically.

The fluctuation operator has been derived previously [33], in the context of quantum corrections to the Abelian instanton; we here recall this derivation. The gauge and Higgs fields are expanded as

$$A^\mu = A_{\text{cl}}^\mu + a^\mu, \tag{3.12}$$

$$\phi = \phi^{\text{cl}} + \varphi. \tag{3.13}$$

In the following we will drop the superscript cl, so the letters A^μ and ϕ will denote the background field, and a^μ and φ the quantum fluctuations.

In order to eliminate the gauge degrees of freedom, we introduce, as in Ref. [36], the background gauge function:

$$\mathcal{F}(a) = \partial_\mu a^\mu - \frac{ig}{2}(\phi^*\varphi - \phi\varphi^*). \tag{3.14}$$

We note that for the background field $\partial^\mu A_\mu = 0$. In the Feynman background gauge we get the gauge-fixing Lagrange density

$$\begin{aligned}\mathcal{L}_{\text{GF}}^{II} &= -\left(\frac{1}{2}\mathcal{F}^2(a)\right)^{II} \\ &= -\frac{1}{2}(\partial_\mu a^\mu)^2 - \frac{ig}{2}a^\mu(\varphi\partial_\mu\phi + \phi\partial_\mu\varphi - \varphi^*\partial_\mu\phi \\ &\quad - \phi\partial_\mu\varphi^*) + \frac{g^2}{8}\phi^2(\varphi - \varphi^*)^2.\end{aligned} \tag{3.15}$$

The associated Faddeev-Popov Lagrangian becomes

$$\mathcal{L}_{\text{FP}} = \tfrac{1}{2}\eta^*(-\partial^2 - g^2\phi^2)\eta. \tag{3.16}$$

In terms of the real components $\varphi = \varphi_1 + i\varphi_2$ and $\eta = (\eta_1 + i\eta_2)$, the second-order Lagrange density now becomes

$$(\mathcal{L}+\mathcal{L}_{\rm GF}+\mathcal{L}_{\rm FP})^{II} = -a_\mu \tfrac{1}{2}(-\Box + g^2\phi^2)a^\mu + \varphi_1 \tfrac{1}{2}[-\Box + g^2 A_\mu A^\mu - \lambda(3\phi^2 - v^2)]\varphi_1 + \varphi_2 \tfrac{1}{2}[-\Box + g^2 A_\mu A^\mu - g^2\phi^2 - \lambda(\phi^2 - v^2)]\varphi_2 + \varphi_2(gA^\mu \partial_\mu)\varphi_1 + \varphi_1(-gA^\mu\partial_\mu)\varphi_2 + a^\mu(2g^2 A_\mu \phi)\varphi_1 + a^\mu(2g\partial_\mu\phi)\varphi_2 + \eta_1 \tfrac{1}{2}(-\Box - g^2\phi^2)\eta_1 + \eta_2 \tfrac{1}{2}(-\Box - g^2\phi^2)\eta_2, \quad (3.17)$$

where we have omitted the superscript from $\phi^{\rm cl}$ and $A_\mu^{\rm cl}$). We now specify the fluctuating fields $(\psi_1, \psi_2, \psi_3, \psi_4, \psi_5)$ as $(a_1^\perp, a_2^\perp, \varphi_1, \varphi_2, \eta_{1,2})$,

$$\begin{pmatrix}\psi_1\\ \psi_2\\ \psi_3\\ \psi_4\\ \psi_5\end{pmatrix} = \begin{pmatrix} a_1^\perp\\ a_2^\perp\\ \varphi_1\\ \varphi_2\\ \eta_{1,2}\end{pmatrix}, \quad (3.18)$$

where we have used Euclidean notation for the transverse gauge field components. The two Faddeev-Popov components η_1 and η_2 have been subsumed into one field, ψ_5, as they have identical fluctuation operators. We furthermore write (see also above)

$$\mathcal{M}_{ij} = (\partial_0^2 - \partial_3^2)\delta_{ij} + \mathcal{M}_{ij}^\perp, \quad (3.19)$$

separating the trivial part from the one that is modified by the background field. With these preliminaries, we obtain the following nonvanishing components of the overall fluctuation operator $\mathcal{M}_{ij}^\perp$:

$$\begin{aligned}
\mathcal{M}^\perp{}_{11} &= -\Delta^\perp + g^2\phi^2 & \mathcal{M}^\perp{}_{22} &= -\Delta^\perp + g^2\phi^2\\
\mathcal{M}^\perp{}_{13} &= 2g^2 A_1^\perp \phi & \mathcal{M}^\perp{}_{14} &= 2g\nabla_1\phi\\
\mathcal{M}^\perp{}_{23} &= 2g^2 A_2^\perp \phi & \mathcal{M}^\perp{}_{24} &= 2g\nabla_2\phi\\
\mathcal{M}^\perp{}_{33} &= -\Delta^\perp + g^2\mathbf{A}^{\perp 2} + g^2\phi^2 + \lambda(\phi^2 - v^2) & \mathcal{M}^\perp{}_{34} &= -g\mathbf{A}^\perp\cdot\nabla\\
\mathcal{M}^\perp{}_{44} &= -\Delta^\perp + g^2\mathbf{A}^{\perp 2} + \lambda(3\phi^2 - v^2) & \mathcal{M}^\perp{}_{43} &= g\mathbf{A}^\perp\cdot\nabla\\
\mathcal{M}^\perp{}_{55} &= -\Delta^\perp + g^2\phi^2.
\end{aligned} \quad (3.20)$$

Owing to the fermionic nature of the Faddeev-Popov ghosts $\eta_{1,2}$, it is understood that the contribution of the operator $\mathcal{M}_{55}$ enters with a factor -2 into the definition of the one-loop string tension. The fluctuation operators for the vortex and vacuum background are now obtained by substituting the corresponding classical fields. The vacuum fluctuation operator becomes a diagonal matrix of Klein-Gordon operators with masses $(\{m_i\}) = (m_W, m_W, m_W, m_H, m_W)$. It is convenient to introduce a potential $\mathcal{V}$ via

$$\mathcal{M}_{ij} = \mathcal{M}_{ij}^0 + \mathcal{V}_{ij}, \quad (3.21)$$

where $\mathcal{M}_{ij}^0 = \delta_{ij}[\Box + m_i^2]$ and where the potential $\mathcal{V}_{ij}$ can be obtained from Eqs. (3.19) and (3.20). It will be explicitly given below, in the partial wave basis.

IV. PARTIAL WAVE DECOMPOSITION

The fluctuation operator $\mathcal{M}^\perp$ can be decomposed into partial waves with respect to the polar angle φ, and the string tension decomposes accordingly. We introduce the following partial wave decomposition for fields:

$$\begin{aligned}
\vec{a} &= \sum_{n=-\infty}^{+\infty} b_n(r)\begin{pmatrix}\cos\varphi\\ \sin\varphi\end{pmatrix}\frac{e^{in\varphi}}{\sqrt{2\pi}} + ic_n(r)\begin{pmatrix}-\sin\varphi\\ \cos\varphi\end{pmatrix}\frac{e^{in\varphi}}{\sqrt{2\pi}},\\
\varphi_1 &= \sum_{n=-\infty}^{+\infty} h_n(r)\frac{e^{in\varphi}}{\sqrt{2\pi}},\\
\varphi_2 &= \sum_{n=-\infty}^{+\infty} \tilde{h}_n(r)\frac{e^{in\varphi}}{\sqrt{2\pi}},\\
\eta_{1,2} &= \sum_{n=-\infty}^{+\infty} g_n(r)\frac{e^{in\varphi}}{\sqrt{2\pi}}.
\end{aligned} \quad (4.1)$$

After inserting these expressions into the Lagrange density and using the reality conditions for the fields, one finds that the following combinations are real relative to each other and make the fluctuation operators symmetric:

$$F_1^n(r) = \tfrac{1}{2}(b_n(r) + c_n(r)), \quad F_2^n(r) = \tfrac{1}{2}(b_n(r) - c_n(r)), \quad F_3^n(r) = \tilde{h}_n(r), \quad F_4^n(r) = ih_n(r), \quad F_5^n(r) = g_n(r). \quad (4.2)$$

Writing the partial fluctuation operators as

$$\mathbf{M}^\perp = \mathbf{M}^\perp{}_0 + \mathbf{V}, \quad (4.3)$$

the free operators $\mathbf{M}^\perp{}_0$ become diagonal matrices with elements

$$M^{\perp}_{0,ii} = -\frac{d^2}{dr^2} - \frac{1}{r}\frac{d}{dr} + \frac{n_i^2}{r^2} + m_i^2, \tag{4.4}$$

where $(n_i) = (n-1, n+1, n, n, n)$ and $(m_i) = (m_W, m_W, m_W, m_H, m_W)$. The potential $\mathbf{V}$ takes the elements

$$\begin{aligned}
\mathbf{V}^n_{11} &= m_W^2(f^2-1) & \mathbf{V}^n_{12} &= 0 \\
\mathbf{V}^n_{13} &= \sqrt{2}m_W f' & \mathbf{V}^n_{14} &= \sqrt{2}m_W f\frac{A+1}{r} \\
\mathbf{V}^n_{22} &= \mathbf{V}^n_{11} & \mathbf{V}^n_{23} &= \mathbf{V}^n_{13} \\
\mathbf{V}^n_{24} &= -\mathbf{V}^n_{14} & \mathbf{V}^n_{33} &= \frac{(A+1)^2}{r^2} + \left(\frac{m_H^2}{2} + m_W^2\right)(f^2-1) \\
\mathbf{V}^n_{34} &= -2\frac{A+1}{r^2}n & \mathbf{V}^n_{44} &= \frac{(A+1)^2}{r^2} + \frac{3}{2}m_H^2(f^2-1) \\
\mathbf{V}^n_{55} &= m_W^2(f^2-1) & \mathbf{V}_{i5} &= 0.
\end{aligned} \tag{4.5}$$

Choosing the dimensionless variable $m_W r$, one realizes that the fluctuation operator only depends on the ratio m_H/m_W up to an overall factor m_W^2 which cancels in the ratio with the free operator.

The fields $A(r)$ and $f(r)$ reach exponentially their asymptotic limits given in Eq. (2.15). As a consequence, it can be verified that the potential $\mathbf{V}^n_{ij}$ is of finite range, and this entails that the computation of the Green's function via mode or Jost functions [22], as described below Eq. (5.10), is mathematically sound. However, one finds a singular behavior at $r = 0$. There the terms $(A+1)^2/r^2$ cause a distortion of the centrifugal barrier for the Higgs fields. This distortion is related to the winding number of the background field. In a suitable diagonalization the effective centrifugal barrier corresponds to $(\bar{n}_i) = (n-1, n+1, n-1, n+1, n)$ instead of the (n_i) given above. This is discussed in some more detail in Refs. [33,34]. At the same time these terms cause the potential not to be square integrable. Had we chosen the regular gauge for the background gauge field, the centrifugal barrier would be determined by (n_i) as $r \to 0$, and the twisted barrier represented by $(\bar{n}_i)$ would determine the behavior as $r \to \infty$. The potential would be long range and again not square integrable; so the difficulties encountered here at $r = 0$ would be transferred to $r \to \infty$, then requiring a modification of the mode function formalism. This explains our preference for the singular gauge.

V. COMPUTATION OF THE EFFECTIVE STRING TENSION

The method for computing the effective string tension used here is based on the Euclidean Green's function of the fluctuation operator. This Green's function is defined by

$$(\nu^2 + k_3^2 + \mathcal{M}^{\perp})\mathcal{G}(\vec{x}_\perp, \vec{x}'_\perp, k_3, \nu) = \mathbf{1}\delta(\vec{x}_\perp - \vec{x}'_\perp), \tag{5.1}$$

and similarly for the operator $\mathcal{M}^0$. It contains the information on the eigenvalues λ_α^2 of the fluctuation operator $\mathcal{M}^{\perp}$ via

$$\int d^2x^{\perp}\,\mathrm{Tr}\mathcal{G}(\vec{x}^{\perp}, \vec{x}^{\perp}, k_3, \nu) = \sum_\alpha \frac{1}{\lambda_\alpha^2 + k_3^2 + \nu^2}. \tag{5.2}$$

We define a function $F(k_3, \nu)$ as

$$\begin{aligned}
F(k_3, \nu) = \int d^2x^{\perp}\,\mathrm{Tr}(&\mathcal{G}(\vec{x}^{\perp}, \vec{x}^{\perp}, k_3, \nu) \\
&- \mathcal{G}^0(\vec{x}^{\perp}, \vec{x}^{\perp}, k_3, \nu)).
\end{aligned} \tag{5.3}$$

We then find

$$\begin{aligned}
-\int_{-\infty}^{\infty}\frac{d\nu\nu^2}{2\pi}F(k_3, \nu) = \sum_\alpha \frac{1}{2}[&\sqrt{k_3^2 + \lambda_\alpha^2} \\
&- \sqrt{k_3^2 + (\lambda_\alpha^{(0)})^2}].
\end{aligned} \tag{5.4}$$

This expression is still to be integrated over k_3 and is by itself already linearly divergent. The sum over eigenvalues becomes an integral $\int d^2k^{\perp}$ and the difference of the energies behaves asymptotically as $1/|k^{\perp}|$. So regularization is required. This will be discussed in the next section. Assuming that it has been achieved, we can do the ν and k_3 integrations at once, using the fact that $F(k_3, \nu)$ only depends on $p = \sqrt{k_3^2 + \nu^2}$, i.e., $F(k_3, \nu) = F(0, p)$. We then obtain for the one-loop string tension

$$\sigma_{\mathrm{fl}} = -\int_0^{\infty}\frac{dpp^3}{4\pi}F(0, p). \tag{5.5}$$

After these more formal considerations we will present the way in which we actually compute $F(k_3, \nu)$. We first use the partial wave decomposition to write

$$F(k_3, \nu) \equiv F(p) = \sum_{n=-\infty}^{+\infty} F_n(p), \tag{5.6}$$

where

$$F_n(p) = \int dr\, r\, \mathrm{Tr}(\mathbf{G}_n(r, r, p) - \mathbf{G}_n^0(r, r, p)), \tag{5.7}$$

and where the partial wave Green functions are defined by

$$(\mathbf{M}_n + p^2)\mathbf{G}_n(r, r', p) = \mathbf{1}\frac{1}{r}\delta(r - r'). \tag{5.8}$$

For $\mathbf{M}_n^0$ the Green function is simply a diagonal matrix with elements

$$\mathbf{G}^{\,0}_{n\,ii}(r, r', p) = I_{n_i}(\kappa_i r_<)K_{n_i}(\kappa_i r_>), \tag{5.9}$$

where $\kappa_i = \sqrt{m_i^2 + p^2}$. For the Green function of the operator $\mathbf{M}_n$ the matrix elements similarly become [19]

$$\mathbf{G}_{\,n\,ij}(r, r', p) = f_{ni}^{\alpha-}(r_<)f_{nj}^{\alpha+}(r_>), \tag{5.10}$$

where the mode functions $f_{ni}^{\alpha\pm}$ form a fundamental system of linearly independent solutions of (5.8), regular as $r \to 0$ for the minus sign and as $r \to \infty$ for the plus sign. For the single channel, this representation of Green's functions by Jost functions can be found in many textbooks, e.g., Ref. [22]. For coupled channels, a derivation can be found in the Appendix of Ref. [37]. The correct normalization is obtained by imposing the boundary conditions

$$f_{ni}^{\alpha-}(r) \simeq \delta_i^\alpha I_{n_i}(\kappa_i r), \qquad f_{ni}^{\alpha+}(r) \simeq \delta_i^\alpha K_{n_i}(\kappa_i r), \tag{5.11}$$

as $r \to \infty$. Actually we have solved numerically the differential equations for the functions $h_i^{\alpha\pm}$ defined by

$$f_{ni}^{\alpha\pm} = B_{n_i}^{\pm}(\kappa_i r)(\delta_i^{\alpha\pm} + h_{ni}^{\alpha\pm}(r)), \tag{5.12}$$

where $B_{n_i}^+ = K_{n_i}$ and $B_{n_i}^- = I_{n_i}$ are the appropriate Bessel functions, and with the boundary conditions $h_{ni}^{\alpha\pm} \to 0$ as $r \to \infty$. In this way, one keeps track of the free contribution $\propto \delta_i^\alpha$ and

$$\begin{aligned}&\mathrm{Tr}[\mathbf{G}_n(r, r, \nu) - \mathbf{G}_n^0(r, r, \nu)]\\ &= [h_{ni}^{i-}(r) + h_{ni}^{i+}(r) + h_{ni}^{\alpha-}(r)h_{ni}^{\alpha+}(r)]I_{n_i}(\kappa_i r)K_{n_i}(\kappa_i r),\end{aligned} \tag{5.13}$$

to be inserted into (5.6). Equations (5.5), (5.6), (5.7), and (5.13) define an exact expression for the one-loop string tension, which, however, has to be renormalized.

VI. RENORMALIZATION

The expression (5.5) for the string tension is divergent. The trace of the Green's function appearing in this definition, see Eq. (5.7), can be expanded perturbatively with respect to the potential $\mathcal{V}$, and one finds that the divergences arise from contributions of first and second order in $\mathcal{V}$. These can be related to the divergences found in standard perturbation theory which can be regularized and renormalized in the usual way. The strategy for renormalization is, therefore, to first subtract the divergent parts from $F(p)$ and then to add back the finite parts remaining after regularization and renormalization. This will be discussed in detail in this section.

The expansion of the Green's function is based on the equations

$$\mathcal{M}\,\mathcal{G}(x, x') = (\mathcal{M}^0 + \mathcal{V})\mathcal{G}(x, x') = \delta^4(x - x') \tag{6.1}$$

and

$$\mathcal{M}^{\,0}\mathcal{G}^0(x, x') = \delta^4(x - x') \tag{6.2}$$

from which we get the standard expansion

$$\begin{aligned}\mathcal{G}_{ii}(x, x) = \mathcal{G}_{ii}^0(x, x) &- \int d^4x' \mathcal{G}_{ii}^0(x, x')\mathcal{V}_{ii}(x')\mathcal{G}_{ii}^0(x', x)\\ &+ \int d^4x' \int d^4x'' \mathcal{G}_{ii}^0(x, x')\mathcal{V}_{ik}(x')\\ &\times \mathcal{G}_{kk}^0(x', x')\mathcal{V}_{ki}(x'')\mathcal{G}_{ii}^0(x'', x) + \cdots,\end{aligned} \tag{6.3}$$

where we have already taken the diagonal elements of Green's function at equal arguments, as needed here. The potential $\mathcal{V}_{ij}$ is a function only of the transversal components of x. We call this expansion of the Green's function the *vertex expansion*, the vertices being given by the components of the potential $\mathcal{V}$. The first two terms in this expansion are represented graphically in Figs. 1 and 2. The Green's functions $\mathcal{G}^0$ are of course just the Feynman propagators and in this form the expansion can be compared easily with the Feynman graph expansion of the effective action. The vertex graphs and the Feynman graphs are not identical, but closely related. In general, the one-vertex graph is a sum of several Feynman graphs. The relation will be presented in detail below, in Secs. (VI A)–(VI F).

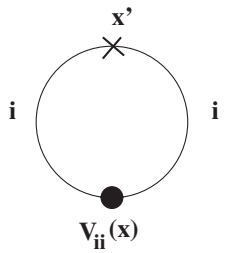

FIG. 1. The one-vertex graph. The cross symbolizes the point where the first-order Green's function is contracted.

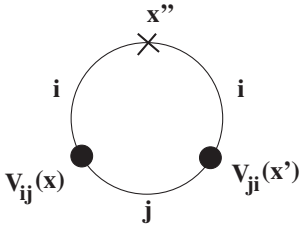

FIG. 2. The two-vertex graph. The cross symbolizes the point where the second-order Green's function is contracted.

Using formulas given in Appendices A, B, and C, the vertex expansion can be formulated in terms of partial waves, and this will be the basis for performing the subtractions numerically.

Our numerical results are computed in such a way that we first compute the contributions of the subsystems for fixed n, then sum over n, and finally integrate over p. The subtractions necessary to make the summation over n and the integration over p convergent are done in the partial waves. There are two ways of doing this: either one plainly subtracts in the partial waves the first-order contributions $\mathrm{Tr}G_n^{(1)} = -\mathrm{Tr}G_n^0 V_{ii} G_n^0$ and the second-order contributions $\mathrm{Tr}G_n^{(2)} = \mathrm{Tr}G_n^0 V_{ij} G_n^0 V_{ji} G_n^0$, or one does the subtractions already in the functions $h_{n,i}^{\alpha\pm}$ as described in detail in Ref. [21]. For the Faddeev-Popov sector we have used both methods and the results agree very well. In the gauge-Higgs sector, the singularity of the external gauge field at $r = 0$ leads to specific difficulties, to be discussed below. These are easier to handle with the first method, and so we decided to work with the plain subtractions throughout.

The essential problems occurring here are twofold: (i) the external gauge field is not square integrable, due to its singularity at $r = 0$, and (ii) there are cancellations between graphs of different order in the external vertices, the well-known cancellation of the quadratic divergence in the vacuum polarization involves seagull terms with one vertex and graphs with two vertices. Such cancellations occur in higher orders as well, so one has to be careful; some contributions with two external vertices do not have to be subtracted, because their divergences are canceled by those of graphs with more than two vertices. These statements apply both to the vertex expansion for the Green's function as also to Feynman graphs with different numbers of vertices.

In the following we will treat the various contributions of first and second order in the vertices term by term, comparing the contributions which are subtracted with the corresponding Feynman graphs. The subtracted contributions are then added back in covariant form. In this way we preserve covariance, which would be violated if we would introduce noncovariant cutoffs (e.g. in p).

The Feynman rules are formulated in the vacuum sector, with a gauge fixing analogous to the one for the vortex

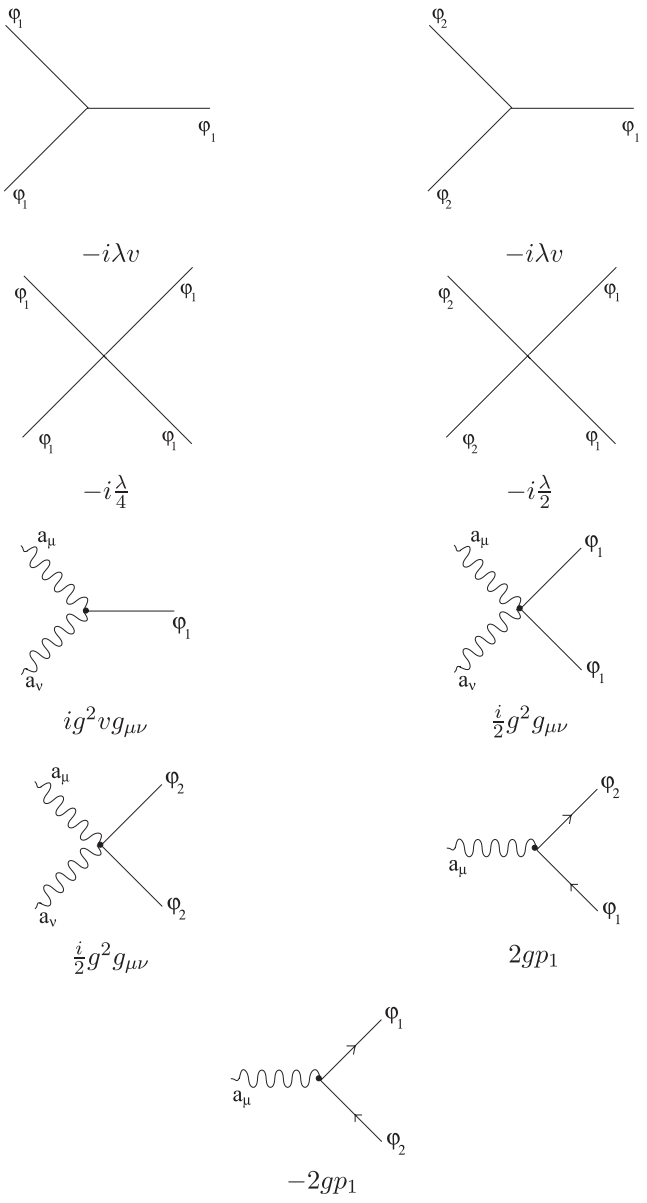

FIG. 3. Vertices for Feynman graphs derived from the Lagrangian (6.6): gauge-Higgs sector. We have not included combinatorial factors for permutations of the external lines.

sector: we define the background gauge function

$$\mathcal{F}_v(A) = \partial_\mu a^\mu - \frac{ig}{2}[(v+\varphi_1)^*\varphi - (v+\varphi_1)\varphi^*] \quad (6.4)$$

and the gauge-fixing Lagrangian

$$\begin{aligned}\mathcal{L}_{\mathrm{GF}}^{II} &= -\left(\frac{1}{2}\mathcal{F}_v^2(A)\right)^{II} \\ &= -\frac{1}{2}(\partial_\mu a^\mu)^2 + g a^\mu(\varphi_2\partial_\mu\varphi_1 + (v+\varphi_1)\partial_\mu\varphi_2) \\ &\quad - \left(\frac{g^2}{2}v^2 + g^2 v\varphi_1 + \frac{g^2}{2}\varphi_1^2\right)\varphi_2^2. \end{aligned} \quad (6.5)$$

Then the Lagrangian, including the gauge fixing and Faddeev-Popov terms, takes the form

$$\mathcal{L} = -\frac{1}{2}\partial_\mu a_\nu \partial^\mu a^\nu + \frac{1}{2}m_W^2 a_\mu a^\mu + \frac{1}{2}\partial_\mu \varphi_1 \partial^\mu \varphi_1 - \frac{1}{2}m_H^2 \varphi_1^2 + \frac{1}{2}\partial_\mu \varphi_2 \partial^\mu \varphi_2 - \frac{1}{2}m_W^2 \varphi_2^2 + 2g a^\mu \varphi_2 \partial_\mu \varphi_1 + g^2 a_\mu a^\mu v \varphi_1 + \frac{1}{2}g^2 a_\mu a^\mu (\varphi_1^2 + \varphi_2^2) - \frac{\lambda}{4}(\varphi_1^4 + \varphi_2^4 + 2\varphi_1^2\varphi_2^2) - \lambda v \varphi_1^3 - \lambda v \varphi_1 \varphi_2^2 - g^2 v \varphi_1 \varphi_2^2 - \frac{g^2}{2}\varphi_1^2\varphi_2^2 + \sum_{i=1}^{2} \eta_i \frac{1}{2}(-\Box - g^2(v+\varphi_1)^2)\eta_i. \tag{6.6}$$

The vertices for the Feynman rules are presented in Figs. 3 and 4.

We denote as Feynman graphs the vacuum graphs with the external sources which are provided by the classical Higgs and gauge fields: $\varphi_1(x) = v[f(r) - 1]$, $\varphi_2 = 0$, $a_\mu = 0$ for $\mu = 0, 1$ and $a_i = \epsilon_{ik}x_k(A(r) + 1)/gr^2$ for $i = 3, 4$. Vacuum graphs with external fields φ_2 will not be displayed as they do not contribute.

A. Graphs with one vertex

The graphs with one vertex all come within a combination analogous to the one displayed in Fig. 5, except for the graphs with the seagull vertex. The external lines $v\phi_1$ and ϕ_1^2 combine as $v^2(f(r) - 1) + v^2(f - 1)^2/2 = v^2(f^2 - 1)/2$. They then are in correspondence with one of the vertex graphs with the external potential $V_{ii}(r)$. In order to illustrate the relation between the Feynman and vertex graphs, we consider the graphs with a Higgs field loop. The corresponding vertex graph is the one with the vertex V_{44}. We use the subscript 44 for identifying this contribution.

The Feynman rules yield the contribution

$$\begin{aligned} &3i\lambda v^2 \frac{m_H^2}{32\pi^2}\left(L_\epsilon + 1 - \ln\frac{m_H^2}{\mu^2}\right) LT \int d^2x \left[(f(r) - 1) + \frac{1}{2}(f(r) - 1)^2\right] \\ &= iLT\frac{3m_H^2}{64\pi^2}\left(L_\epsilon + 1 - \ln\frac{m_H^2}{\mu^2}\right)\int d^2x[f^2(r) - 1] \\ &\equiv -iLT\Delta\sigma_{\mathrm{fl},44}, \end{aligned} \tag{6.7}$$

where $L_\epsilon = 2/\epsilon - \gamma + \ln 4\pi$ and where we have used $\lambda v^2 = m_H^2/2$. The factor LT comes from the trivial integrations over time and along the string axis. The Feynman graph constitutes a correction to iS, where S is the action, so as an energy correction it receives a minus sign.

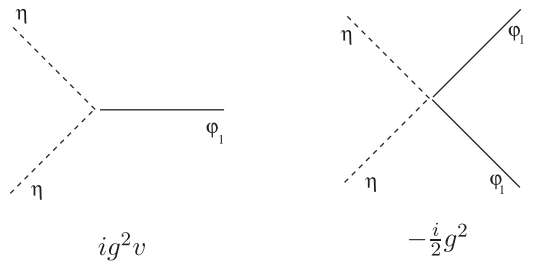

FIG. 4. Vertices for Feynman graphs derived from the Lagrangian (6.6): Faddeev-Popov sector, without combinatorial factors for permutations of external lines.

The contribution we subtract is given, in the partial waves, by

$$F_{44}^n = -\int_0^\infty r dr \int_0^\infty r' dr' V_{44}^H(r) G_n^0(r, r', \kappa_H) G_n^0(r', r, \kappa_H). \tag{6.8}$$

The corresponding vertex graph is of the type shown in Fig. 1. As announced above, we do not include the $(A(r) + 1)^2/r^2$ term and denote the restricted potential by V_{44}^H. We also leave out the index n as this potential does not depend on it. The r' integration can be carried out and one finds

$$F_{n,44} = \frac{d}{dm_H^2}\int_0^\infty r dr V_{44}(r) G_n^0(r, r, \kappa_H). \tag{6.9}$$

This can be summed up to yield

$$\begin{aligned} F_{44}(p) &= \frac{d}{dm_H^2} 2\pi \int_0^\infty r dr V_{44}^H(r) G^0(\mathbf{x}, \mathbf{x}, \kappa_H) \\ &= \frac{1}{2p}\frac{d}{dp}\int \frac{d^2k}{(2\pi)^2}\frac{1}{\mathbf{k}^2 + p^2 + m_H^2}\int d^2x V_{44}^H(r). \end{aligned} \tag{6.10}$$

This is discussed in some more detail in Appendix B. Integration over $dpp^3/4\pi$ leads, after integration by parts, to

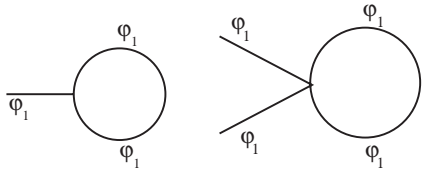

FIG. 5. Feynman graphs corresponding to the one-vertex graph with V_{44}^H.

$$\Delta\sigma_{\mathrm{fl},44} = -\int_0^\infty \frac{p^3 dp}{4\pi} F_{44}(p)$$
$$= \int_0^\infty \frac{p dp}{4\pi} \frac{d^2k}{(2\pi)^2} \frac{1}{k^2 + p^2 + m_H^2} \int d^2x V_{44}^H(r)$$
$$= \frac{1}{2} \int \frac{d\nu dk_3 d^2k}{(2\pi)^4} \frac{1}{\mathbf{k}^2 + k_3^2 + \nu^2 + m_H^2} \times \int d^2x V_{44}^H(r). \quad (6.11)$$

If we use dimensional regularization applied to the Euclidean four momentum integration $d\nu dk_3 d^2k = d^4k$, we obtain

$$\Delta\sigma_{\mathrm{fl},44} = -\frac{m_H^2}{32\pi^2}\left[L_\epsilon + 1 - \ln\frac{m_H^2}{\mu^2}\right]\int d^2x V_{44}^H(r)$$
$$= -3\frac{m_H^4}{64\pi^2}\left[L_\epsilon + 1 - \ln\frac{m_H^2}{\mu^2}\right]\int d^2x (f^2(r) - 1) \quad (6.12)$$

in agreement with the result from the Feynman graph. In this case it was possible to check in detail the relation between the subtracted part, the vertex graph, and the Feynman graphs.

Obviously the procedure is analogous for the other graphs with one vertex. We obtain, both by using the Feynman graphs of Fig. 6 as well as from the vertex graph:

$$\Delta\sigma_{\mathrm{fl},33} = -\frac{m_H^2}{32\pi^2}\left[L_\epsilon + 1 - \ln\frac{m_W^2}{\mu^2}\right]\int d^2x V_{33}^H(r)$$
$$= -(m_H^2 + 2m_W^2)\frac{m_H^2}{64\pi^2}\left[L_\epsilon + 1 - \ln\frac{m_W^2}{\mu^2}\right] \times \int d^2x (f^2(r) - 1). \quad (6.13)$$

For the contribution of V_{11} and V_{12} in the sector of angular momentum n, one notes that they involve the Green's functions $G^0_{n\pm1}$. In the sum the shifts compensate each other and the result is, both from the Feynman graphs in Fig. 7 as well as from the vertex graphs,

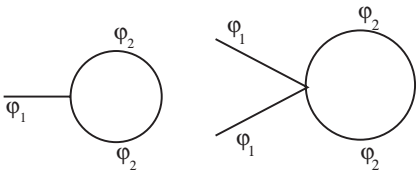

FIG. 6. Feynman graphs corresponding to the one-vertex graph with V_{33}^H.

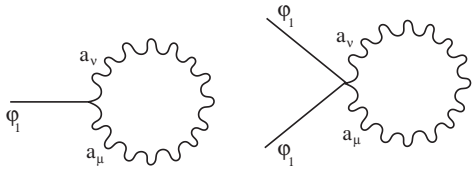

FIG. 7. Feynman graphs corresponding to the one-vertex graphs with V_{11} and V_{22}.

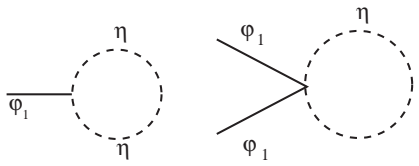

FIG. 8. Feynman graphs corresponding to the one-vertex graph with V_{55}.

$$\Delta\sigma_{\mathrm{fl},11+22} = -\frac{m_W^2}{32\pi^2}\left[L_\epsilon + 1 - \ln\frac{M_W^2}{\mu^2}\right] \times \int d^2x [V_{11}(r) + V_{22}(r)]$$
$$= -\frac{m_W^4}{16\pi^2}\left[L_\epsilon + 1 - \ln\frac{m_W^2}{\mu^2}\right] \times \int d^2x (f^2(r) - 1). \quad (6.14)$$

These are canceled exactly by the Faddeev-Popov graphs of Fig. 8.

B. Graphs with two vertices: $V_{ii} \times V_{ii}$

We have subtracted in the partial waves the second-order contributions to $\mathcal{F}_n^{(2)}(p)$ of the type

$$F_{n,ij,ji}(p) = \int dr' r' \int dr r \int dr'' r'' V_{ij}(r) G_n^0(r, r', \kappa_j) \times V_{ji}(r') G_n^0(r', r'', \kappa_i) G_n^0(r'', r, \kappa_i), \quad (6.15)$$

as represented graphically in Fig. 2. The r'' integration can be done, see Appendix C, with the result

$$F_{n,ij,ji}(p) = -\frac{d}{dm_i^2} \int dr' r' \int dr r V_{ij}^n(r) G_n^0(r, r', \kappa_j) \times V_{ji}^n(r') G_n^0(r', r, \kappa_i). \quad (6.16)$$

We recall that $\kappa_j^2 = p^2 + m_j^2$. The one-to-one relation with Feynman graphs is most obvious for the diagonal parts where $i = j$, and we will treat these first. For V_{33} and V_{44} we again discard the gauge field parts $V_{33}^g = V_{44}^g = (A(r) + 1)/r^2$, restricting them to the Higgs field contributions V_{33}^H and V_{44}^H This will be justified later. As now $\kappa_i = \kappa_j$, we can apply the derivative with respect to m_i^2 to both Green's functions and compensate this double action by a

factor $1/2$. Furthermore, we can replace this derivative by the derivative with respect to $dp^2 = 2pdp$, applied to the whole graph. Then

$$\begin{aligned}-\int\frac{dp}{4\pi}p^3F_{n,ii,ii}(p) &= \frac{1}{2}\int\frac{p^3dp}{4\pi}\frac{1}{2p}\frac{d}{dp}\int dr'r'\\ &\quad\times\int drrV_{ii}^n(r)G_n^0(r,r',\kappa_i)V_{ii}^n(r')\\ &\quad\times G_n^0(r',r,\kappa_i)\\ &= -\int\frac{pdp}{8\pi}\int dr'r'\int drrV_{ii}^n(r)\\ &\quad\times G_n^0(r,r',\kappa_i)V_{ii}^n(r')G_n^0(r',r,\kappa_i).\end{aligned} \tag{6.17}$$

As the potentials under consideration do not depend on n we may sum over n to obtain

$$\begin{aligned}&-\int\frac{pdp}{8\pi}\int d^2x\int d^2x'V_{ii}(r)G^0(\mathbf{x},\mathbf{x}',\kappa_i)V_{ii}(r')\\ &\quad\times G^0(\mathbf{x}',\mathbf{x},\kappa_i),\end{aligned} \tag{6.18}$$

and this is just the conventional Feynman graph with external sources. As in the case with one vertex the integral over $pdp/2\pi$ can be rewritten as an integral over $dk_3d\nu/(2\pi)^2$, and the Green's function G^0 in two dimensions involves the integral over $dk_\perp^2$, so altogether we have an integration over $d^4k/(2\pi)^4$, times a factor $1/4$. In momentum space we obtain

$$\begin{aligned}&-\frac{1}{4}\int\frac{d^2q}{(2\pi)^2}|\tilde{V}_{ii}(q)|^2\int\frac{d^4k}{(2\pi)^4}\\ &\quad\times\frac{1}{[k^2+m_i^2][(k+q)^2+m_j^2]},\end{aligned} \tag{6.19}$$

where $q = (0,0,\mathbf{q})$ has only the transversal components.

The Euclidean Feynman integral is logarithmically divergent. In dimensional regularization it is given by

$$\begin{aligned}&\int\frac{d^{4-\epsilon}k}{(2\pi)^{4-\epsilon}}\frac{1}{[k^2+m_i^2][(k+q)^2+m_j^2]}\\ &=\frac{1}{16\pi^2}\Big\{L_\epsilon-\int_0^1d\omega\\ &\quad\times\ln\frac{\omega(1-\omega)\mathbf{q}^2+\omega m_i^2+(1-\omega)m_j^2}{\mu^2}\Big\}.\end{aligned} \tag{6.20}$$

This is to be folded with the Fourier transform of f^2-1:

$$[f^2-1]^\sim(\mathbf{q}) = 2\pi\int_0^\infty drr(f^2(r)-1)J_0(qr)\equiv\chi_{f^2-1}(q). \tag{6.21}$$

Altogether we find

$$\begin{aligned}\Delta\sigma_{\mathrm{fl},44,44} &= -\frac{9m_H^4}{256\pi^2}\int\frac{d^2q}{(2\pi)^2}\Big\{L_\epsilon\\ &\quad-\int_0^1d\omega\ln\frac{\omega(1-\omega)\mathbf{q}^2+m_H^2}{\mu^2}\Big\}|\chi_{f^2-1}(q)|^2.\end{aligned} \tag{6.22}$$

The corresponding Feynman graphs are displayed in Fig. 9. The external legs combine as

$$\begin{aligned}&18\lambda^2v^4[(f(r)-1)(f(r')-1)+(f(r)-1)^2(f(r')-1)/2\\ &\quad+(f(r)-1)(f(r')-1)^2/2\\ &\quad+(f(r)-1)^2(f(r')-1)^2/4]\\ &=(9/2)\lambda^2v^4(f^2(r)-1)(f^2(r')-1)\\ &=(9/8)m_H^4(f^2(r)-1)(f^2(r')-1).\end{aligned} \tag{6.23}$$

Using the $\overline{MS}$ scheme the finite contribution is given by

$$\begin{aligned}\Delta\sigma_{\mathrm{fl},44,44} &= \frac{9m_H^4}{256\pi^2}\int\frac{d^2q}{(2\pi)^2}\\ &\quad\times\int_0^1d\omega\ln\frac{\omega(1-\omega)\mathbf{q}^2+m_H^2}{\mu^2}|\chi_{f^2-1}(q)|^2.\end{aligned} \tag{6.24}$$

The integral over the logarithm is discussed in Appendix G. The Fourier transform of the potential, which actually is a Fourier-Bessel transform, is discussed in Appendix F. The analogous diagonal contributions, displayed in Figs. 10–12, are given by

$$\begin{aligned}\Delta\sigma_{\mathrm{fl},33,33} &= \frac{(m_W^2+m_H^2/2)^2}{64\pi^2}\int\frac{d^2q}{(2\pi)^2}\\ &\quad\times\int_0^1d\omega\ln\frac{\omega(1-\omega)\mathbf{q}^2+m_W^2}{\mu^2}|\chi_{f^2-1}(q)|^2,\end{aligned} \tag{6.25}$$

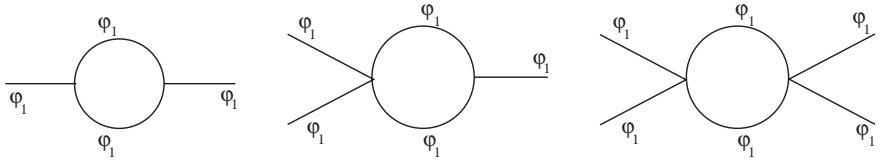

FIG. 9. Feynman graphs corresponding to the vertex graph with $V_{44}^H\times V_{44}^H$.

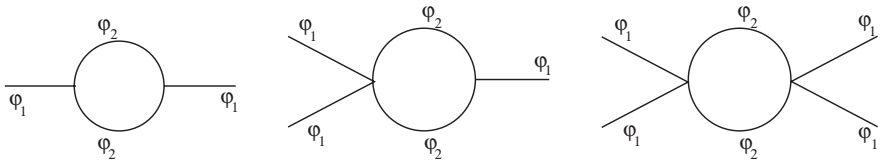

FIG. 10. Feynman graphs corresponding to the vertex graph with $V_{33}^H \times V_{33}^H$.

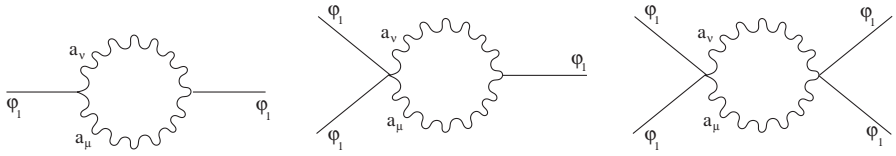

FIG. 11. Feynman graphs corresponding to the vertex graphs with $V_{11} \times V_{11}$ and $V_{22} \times V_{22}$.

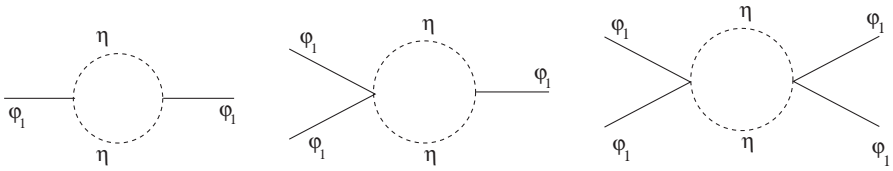

FIG. 12. Feynman graphs corresponding to the Faddeev-Popov ghost vertex graphs with $V_{55} \times V_{55}$.

$$\Delta\sigma_{\mathrm{fl},11,11} + \Delta\sigma_{\mathrm{fl},22,22} = \frac{m_W^4}{32\pi^2}\int\frac{d^2q}{(2\pi)^2} \times \int_0^1 d\omega \ln\frac{\omega(1-\omega)\mathbf{q}^2 + m_H^2}{\mu^2} \times |\chi_{f^2-1}(q)|^2, \quad (6.26)$$

and

$$\Delta\sigma_{\mathrm{fl},55,55} = -\frac{m_W^4}{32\pi^2}\int\frac{d^2q}{(2\pi)^2} \times \int_0^1 d\omega \ln\frac{\omega(1-\omega)\mathbf{q}^2 + m_H^2}{\mu^2}|\chi_{f^2-1}(q)|^2, \quad (6.27)$$

respectively. The latter two contributions, those of the transverse gauge field and the Faddeev-Popov fluctuations, cancel each other, as for the first-order contributions.

C. Graphs with two vertices: $V_{13} \times V_{31}$ and $V_{23} \times V_{32}$

The vertex graphs with $V_{13} \times V_{31}$ and $V_{23} \times V_{32}$ correspond to the Feynman graph of Fig. 13. The Feynman integral is given by

$$-\frac{ig^2}{8\pi^2}q^2\left\{L_\epsilon - \int_0^1 d\omega \ln\frac{-\omega(1-\omega)q^2 + m_W^2}{\mu^2}\right\}. \quad (6.28)$$

The external legs are given by $v(f-1)$. Denoting the Fourier transform by

$$[v(f-1)]^{\sim}(\mathbf{q}) \equiv v\chi_{f-1}(q) = 2\pi v\int_0^\infty dr r(f(r)-1)J_0(qr) \quad (6.29)$$

we obtain for the Feynman graph including the external legs

$$iLT\frac{m_W^2}{8\pi^2}\int\frac{d^2q}{(2\pi)^2}\mathbf{q}^2|\chi_{f-1}(q)|^2 \times \left\{L_\epsilon - \int d\omega \ln\frac{\omega(1-\omega)\mathbf{q}^2 + m_W^2}{\mu^2}\right\}. \quad (6.30)$$

The infinite part corresponds to the wave function renormalization of the Higgs field. In the $\overline{MS}$ scheme, the finite correction to the string tension is given by

$$\Delta\sigma_{\mathrm{fl},(12)3,(12)3} = \frac{m_W^2}{8\pi^2}\int\frac{d^2q}{(2\pi)^2}\mathbf{q}^2|\chi_{f-1}(q)|^2 \times \int d\omega \ln\frac{\omega(1-\omega)\mathbf{q}^2 + m_W^2}{\mu^2}. \quad (6.31)$$

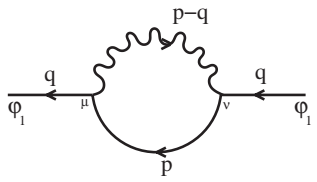

FIG. 13. Feynman graph corresponding to the vertex graphs with $V_{13} \times V_{31}$ and $V_{23} \times V_{32}$.

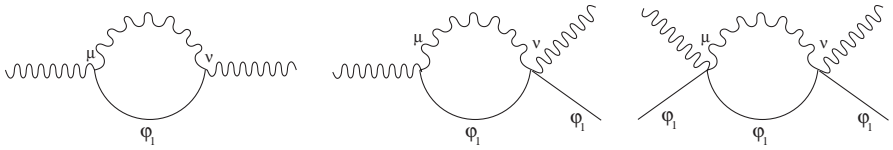

FIG. 14. The Feynman graphs corresponding to the vertex graphs with $V_{14} \times V_{41}$ and $V_{24} \times V_{42}$.

D. Graphs with two vertices: $V_{14} \times V_{41}$ and $V_{24} \times V_{42}$

These nondiagonal terms correspond to the Feynman graphs of Fig. 14. The external Higgs field legs combine as

$$1 + (f(r) - 1) + (f(r') - 1) + (f(r) - 1)(f(r') - 1) = f(r)f(r'). \tag{6.32}$$

The Feynman integral is given by

$$-ig_{\mu\nu}\frac{g^4}{4\pi^2} \times \left\{L_\epsilon - \int_0^1 d\omega \ln\frac{\omega(1-\omega)\mathbf{q}^2 + \omega m_W^2 + (1-\omega)m_H^2}{\mu^2}\right\}. \tag{6.33}$$

The external legs combine to $A_\mu\phi$, which restricts to a two-dimensional vector $A_i^\perp \upsilon f(r)$. We write the Fourier transform as

$$[A_i^\perp \upsilon f]_i^\sim = 2\pi\frac{\upsilon}{g}\epsilon_{ij}\hat{q}_j\int_0^\infty dr(A(r)+1)f(r)J_1(qr) = \frac{\upsilon}{g}\epsilon_{ij}\hat{q}_j\chi_{Af}(q). \tag{6.34}$$

The Feynman graph with external legs then is given by

$$iLT\frac{m_W^2}{8\pi^2}\int\frac{d^2q}{(2\pi)^2}|\chi_{Af}(q)|^2 \times \left\{L_\epsilon - \int_0^1 d\omega \ln\frac{\omega(1-\omega)\mathbf{q}^2 + \omega m_W^2 + (1-\omega)m_H^2}{\mu^2}\right\}. \tag{6.35}$$

The infinite term corresponds to the coupling constant renormalization in the term $g^2|\phi|^2 A_\mu A^\mu/2$. For the finite correction to the string tension we obtain

$$\Delta\sigma_{\mathrm{fl},(12)4,(12)4} = \frac{m_W^2}{8\pi^2}\int\frac{d^2q}{(2\pi)^2}|\chi_{Af}(q)|^2\int_0^1 d\omega \times \ln\frac{\omega(1-\omega)\mathbf{q}^2 + \omega m_W^2 + (1-\omega)m_H^2}{\mu^2}. \tag{6.36}$$

E. Graphs with two vertices: $V_{34} \times V_{43}$

The graphs containing $V_{34} \times V_{43}$ were the hardest stumbling block for this computation. As is well known, the quadratic divergence of the second-order Feynman graph of Fig. 15 cancels with the one of the first-order seagull diagrams displayed in the same figure. The problem we have here is the fact that the quadratic divergence is proportional to $A_\mu A^\mu$ and this has a nonintegrable singularity at $r = 0$. While the ultraviolet divergence appears only after summation over n and integration over p, the radial integrations already appear in the partial waves. On the other hand, all we have to ensure is the fact that the final ultraviolet divergence is a wave function renormalization and does not contain terms proportional to $A_\mu A^\mu$. Furthermore our subtraction must render the total result finite. The solution of this problem was found essentially by trial and error and amounts to subtracting in the partial waves a second-order term

$$\int rdr\int r'dr' V_{34}(r)G_n^0(r,r',\kappa_W)\left[V_{43}(r') - \frac{r^2}{r'^2}V_{43}(r)\right] \times [G_n^0(r',r,\kappa_H)]^2 = \int rdr\int r'dr' 2n\frac{(A(r)+1)}{r^2}G_n^0(r,r',\kappa_W)2n \times \frac{(A(r')-A(r))}{r'^2}[G_n^0(r',r,\kappa_H)]^2, \tag{6.37}$$

and analogously for $V_{43} \times V_{34}$ or $\kappa_W \leftrightarrow \kappa_H$. *This contains already the subtraction of first-order divergences* that would arise from the gauge field parts of V_{33} and V_{44}. So the numerical results get finite *without subtraction of those first-order terms*. However, this subtraction does not cor-

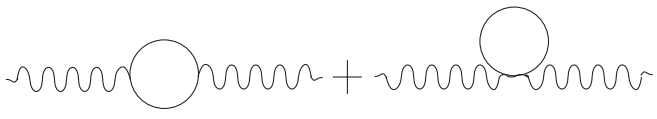

FIG. 15. Vacuum polarization Feynman graphs. They are equivalent to the vertex graphs with $V_{34} \times V_{43}$ and $V_{43} \times V_{34}$, and to the one-vertex graphs with V_{33}^g and V_{44}^g, respectively.

respond exactly to the subtraction of the Feynman graphs of Fig. 15, it only takes care in the correct way of the divergent terms. The finite terms will be different. So when we add back the subtracted term after covariant regularization, we have to compute it *in the same way as we did the subtraction*, not by evaluating the Feynman graphs with the external gauge field legs. This we will describe now.

The Feynman integral corresponding to the second-order diagram is given, in our gauge, by

$$g^2 \int \frac{d^4p}{(2\pi)^4} \frac{4p_\mu p_\nu}{(p^2 - m_H^2 + i\epsilon)((p-q)^2 - m_W^2 + i\epsilon)}, \tag{6.38}$$

where q_μ is the external momentum. The graph evaluates to

$$i\frac{g^2}{4\pi^2}\int_0^1 d\omega\Big[\frac{2\mathcal{Q}^2}{4-\epsilon}\Big\{L_\epsilon + \frac{1}{2} - \ln\frac{\mathcal{Q}^2}{\mu^2}\Big\} + q_\mu q_\nu \omega^2\Big\{L_\epsilon - \ln\frac{\mathcal{Q}^2}{\mu^2}\Big\}\Big], \tag{6.39}$$

with $\mathcal{Q}^2 = \omega m_W^2 + (1-\omega)m_H^2 - \omega(1-\omega)q^2$. Our gauge potential is transverse, so in the following we do not have to keep track of the $q_\mu q_\nu$ terms. The external fields as we have used them in the subtraction can be written as

$$\epsilon_{ik}\hat{x}_k\epsilon_{jl}\hat{x}_l \frac{A(r)+1}{gr}\frac{A(r')-A(r)}{gr'} = \epsilon_{ik}\hat{x}_k\epsilon_{jl}\hat{x}_l\Big[\frac{A(r)+1}{gr}\frac{A(r')-1}{gr'} - \frac{(A(r)+1)^2}{gr}\frac{1}{gr'}\Big]. \tag{6.40}$$

Taking the Fourier transform and setting $q = q'$ because of momentum conservation, we have

$$\frac{1}{g^2}\epsilon_{ik}\hat{q}_k\epsilon_{jl}\hat{q}_l(2\pi)^2\Big[\int drJ_1(qr)(A(r)+1)\int dr'J_1(qr')\times(A(r')+1) - \int drJ_1(qr)(A(r)+1)^2\int dr'J_1(qr')\Big]. \tag{6.41}$$

Contracting with $g_{\mu\nu}$ we have

$$-\frac{1}{g^2}(2\pi)^2\Big[\int drJ_1(qr)(A(r)+1)\int dr'J_1(qr')(A(r')+1) - \int drJ_1(qr)(A(r)+1)^2\int dr'J_1(qr')\Big]. \tag{6.42}$$

At first we consider the divergent part of the Feynman graph. It is given by

$$i\frac{g^2}{16\pi^2}g_{\mu\nu}L_\epsilon\Big[\frac{1}{3}q^2 - (m_H^2 + m_W^2)\Big]. \tag{6.43}$$

This is to be multiplied with the external leg factor given above and to be integrated with $d^2q/(2\pi)^2$. The part independent of q^2 vanishes upon this integration:

$$\int qdq\Big[\int drJ_1(qr)(A(r)+1)\int dr'J_1(qr')(A(r')+1) - \int drJ_1(qr)(A(r)+1)^2\int dr'J_1(qr')\Big] = \Big[\int dr(A(r)+1)\int dr'(A(r')+1) - \int dr(A(r)+1)^2\int dr'\Big]\frac{1}{r}\delta(r-r') = 0, \tag{6.44}$$

where we have used

$$\int qdqJ_n(qr)J_n(qr') = \frac{1}{r}\delta(r-r'). \tag{6.45}$$

This cancellation implies, as it should, the absence of a divergent term proportional to $A_\mu A^\mu$ in our subtraction. The remaining divergent term is proportional to q^2. We note that now $q^2 = -\mathbf{q}^2$. Furthermore, $\int drJ_1(qr) = 1/q$, $\int dqq^2J_1(qr) = 0$, and $qJ_1(qr) = -dJ_0(qr)/dr$. Including all factors we find

$$i\frac{L_\epsilon}{16\pi^2}\frac{1}{3}2\pi\int q^3dq\Big[\int drJ_1(qr)(A(r)+1)\int dr'J_1(qr')(A(r')+1) - \frac{1}{q}\int drJ_1(qr)(A(r)+1)^2\Big] = i\frac{L_\epsilon}{16\pi^2}\frac{1}{3}2\pi\int qdq\int dr\frac{dJ_0(qr)}{dr}(A(r)+1)\int dr'\frac{dJ_0(qr')}{dr'}(A(r')+1) = i\frac{L_\epsilon}{16\pi^2}\frac{1}{3}2\pi\int\frac{dr}{r}[A'(r)]^2. \tag{6.46}$$

This is just the kinetic term of the gauge field, multiplied with the wave function renormalization factor $(g^2/3)L_\epsilon/8\pi^2$. In the $\overline{MS}$ scheme this term is dropped. We are left with the finite part. Denoting

$$2\pi \int dr J_1(qr)(A(r)+1) = \chi_A(q), \tag{6.47}$$

$$2\pi \int dr J_1(r)(A(r)+1)^2 = \chi_{A^2}(q), \tag{6.48}$$

the finite part is given by

$$\Delta\sigma_{\mathrm{fl},34,34} = \frac{1}{8\pi^2}\int \frac{d^2q}{(2\pi)^2}\int_0^1 d\omega\, \mathcal{Q}^2\left[\ln\frac{\mathcal{Q}^2}{\mu^2} - 1\right] \times\left[\chi_A^2(q) - \frac{2\pi}{q}\chi_{A^2}(q)\right], \tag{6.49}$$

with $\mathcal{Q}^2 = \omega m_H^2 + (1-\omega)m_W^2 + \omega(1-\omega)\mathbf{q}^2$. The integration over $d\omega$ can be done analytically, we do not display the somewhat lengthy result.

F. Graphs with two vertices: gauge field contributions in V_{33} and V_{44}

There are some contributions with two vertices which we have left out. Denoting the gauge part of V_{33} with V_{33}^g with $V_{33}^g(r) = (A(r)+1)^2/r^2$ and analogously for V_{44}, we have left out second order the diagonal parts $V_{33}^g \times V_{33}^H$ and $V_{33}^g \times V_{33}^g$, and likewise for the 44 (Higgs) channel. These diagrams with seagull-type vertices combine with higher order graphs to give finite results. So *they do not have to be subtracted*. The corresponding Feynman graphs are displayed in Figs. 16 and 17. If one looks at the Feynman graphs there are graphs with more than three vertices that are superficially divergent. In fact these combine in such a way that their divergences are canceled. So with the subtractions described in the previous subsections, we have done the necessary steps towards computing the finite result. Indeed with these subtractions the numerical results get finite, and we have already presented the finite expressions by which these graphs are to be replaced.

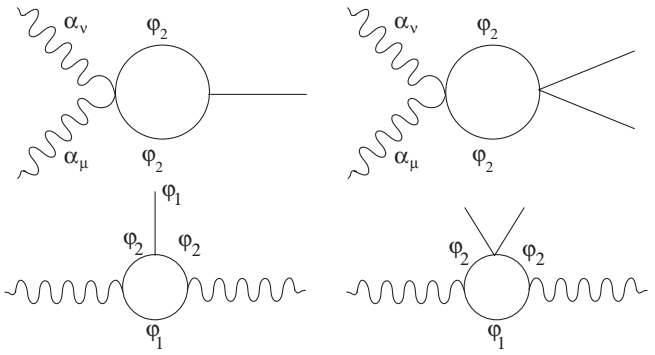

FIG. 16. Feynman graphs corresponding to the vertex graph with $V_{33}^g \times V_{33}^H$ and the three-vertex graphs that cancel their logarithmic divergences. The cancellation for the graphs related to $V_{44}^g \times V_{44}^H$ is analogous, with the replacement $\phi_1 \to \varphi_2$ in the internal lines.

VII. NUMERICAL RESULTS

We have carried out the numerical program as described in the previous sections, for values of $\xi = m_H/m_W$ between 0.5 and 2.

The program starts with computing a fundamental system of the mode functions $h_{n,i}^{\alpha\pm}(r)$ for the 4×4 gauge-Higgs and the Faddeev-Popov sector. We have used 2000 grid points in r, up to $r_{\max} = 30$, as we did already for the classical profiles $f(r)$ and $A(r)$. These are the basis for the partial wave Green's functions. This computation is identical to the one performed already in Refs. [33,34].

We have computed the partial wave Green's function and the related integrals up to $n = \bar{n} = 35$. Contributions of higher n were included by fitting the data between $\bar{n}-5$ and $\bar{n}$ using power fits $An^{-3} + Bn^{-4} + Cn^{-5}$, and by appending the sum for $\bar{n} < n < \infty$ on the basis of these fits. The perturbative subtractions were done in the partial waves, the sum over the unsubtracted and the subtracted partial wave contributions constitute the unsubtracted and subtracted functions $F(p)$. These are displayed, for $\xi = 1$ in Figs. 18 and 19, for the gauge-Higgs and the Faddeev-Popov sector, respectively. All the general features of these figures are similar for other values of ξ. In these figures we also present the perturbative contributions of first and second order, summed separately. These can and have been used for cross-checks against semianalytical results:

The numerical sum over the first-order subtractions can be checked against the result obtained by summing the partial wave contributions analytically. One finds

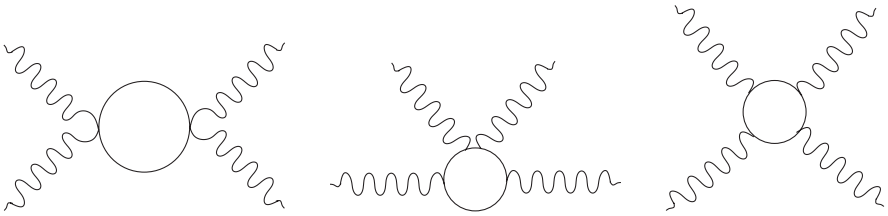

FIG. 17. Feynman graphs corresponding to the vertex graphs with $V_{33}^g \times V_{33}^g$ and $V_{44}^g \times V_{44}^g$ and the higher order graphs that cancel their logarithmic divergences.

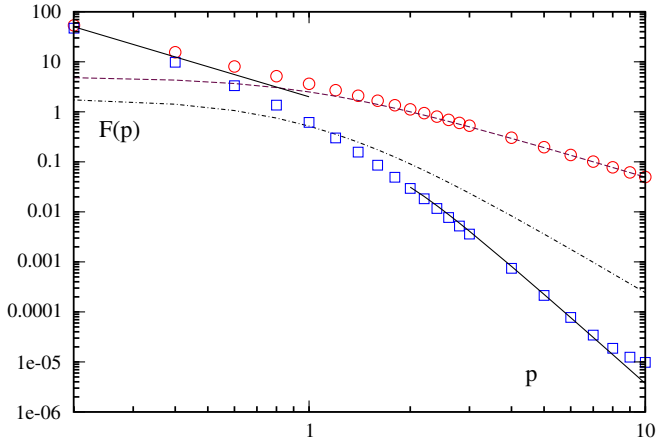

FIG. 18 (color online). The integrand function $F(p)$ defined in Eq. (5.6), for the gauge-Higgs sector: circles, the unsubtracted function; dashed line, one-vertex contribution; dash-dotted line, two-vertex contribution; squares, subtracted function; straight line at small p, translation mode pole $2/p^2$; solid line at large p, asymptotic fit.

$$\sum_{i=1,4} F_{ii}(p) = -\left[\frac{3m_W^2 + m_H^2/2}{2\kappa_W^2} + \frac{3m_H^2/2}{2\kappa_H^2}\right] \times \int rdr(f^2(r) - 1). \tag{7.1}$$

The Faddeev-Popov contribution, which was computed separately, behaves (including the factor -2) as

$$F_{55}(p) = \frac{m_W^2}{\kappa_W^2} \int rdr(f^2(r) - 1). \tag{7.2}$$

The integrals over r, here and below, are computed numerically using the classical profiles.

For the second-order contributions, we cannot do the sum over partial waves analytically, this involves the numerical Fourier transforms of various functions of the classical profiles; but we can easily check the asymptotic behavior. It is given by

$$\sum_{ij} F_{ijij}(p) = \Big[(m_W^4 + (m_W^2 + m_H^2/2)^2 + 9m_H^4/4) \times \int rdr(f^2(r) - 1)^2 + 8m_W^2 \int rdrf'(r)^2 + 8m_W^2 \int rdrf^2(r)\frac{(A(r) + 1)^2}{r^2} + 4\int rdr\frac{[A'(r)]^2}{r^2}\Big]\frac{1}{4p^4}. \tag{7.3}$$

The first term collects the diagonal contributions that can be derived analytically by summing up the partial waves. The three other contributions are retrieved from the Feynman graphs by doing the transverse loop momentum integrations only. They collect the 1313 and 2323 contributions, the 1414 and 2424 contributions, and the 3434 contribution, respectively. Of course these can also be computed and verified separately. The asymptotic behavior of the Faddeev-Popov contribution is given by

$$F_{5555}(p) = 2\frac{m_W^4}{4p^4} \int rdr(f^2(r) - 1)^2. \tag{7.4}$$

These semianalytic results can be and have been checked against the numerical subtractions, thus verifying prefactors and signs.

After the subtractions, the function $F_{\text{sub}}(p)$ behaves as p^{-6} and the integral over p^4dp can be done in order to obtain the subtracted part of the string tension. Finally, we have to add back the subtracted terms in a covariantly regularized and renormalized form given in the previous section.

As we have already mentioned, the integrands for the p integration are displayed in Figs. 18 and 19, for the gauge-Higgs and the Faddeev-Popov sector, respectively. The figures show the unsubtracted functions, the first-order and second-order contributions and the subtracted functions. Note that the functions differ, at large p, by several orders of magnitude, so these subtractions are quite delicate.

The gauge-Higgs sector displays a $2/p^2$ behavior for small p, which is of course related to the 2 translation modes of the two-dimensional solution (the ''instanton''). Here it merges into a continuum of transverse string oscillations. The small-p pole remains of course after subtractions and causes the gauge-Higgs sector to be much more important than the Faddeev-Popov sector. Indeed, the finite parts obtained after integration with $p^3dp/4\pi$ are much larger for the gauge-Higgs than for the Faddeev-Popov sector. Obviously this important contribution of the translation mode is related to the transversal quantum oscillation of the string.

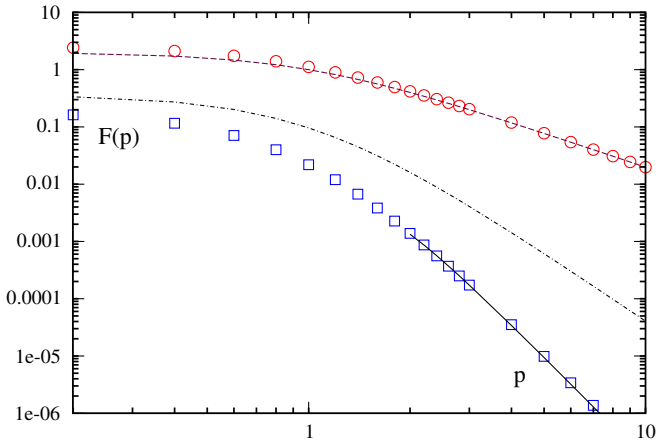

FIG. 19 (color online). The integrand function $F(p)$ defined in Eq. (5.6), for the Faddeev-Popov sector. Symbols and lines as in Fig. 18, except that there is no translation mode pole at small p.

TABLE I. The correction to the string tension as a function of $\xi = m_H/m_W$. We present the finite part of the contributions with one vertex, $\Delta\sigma^{(1)}_{\rm fin}$, the finite contributions from graphs with two vertices $\Delta\sigma^{(2)}_{\rm fin}$, the sum of higher order terms $\Delta\sigma_{\rm sub}$, and the total one-loop correction $\Delta\sigma_{\rm tot}$. We also include the classical string tensions. All entries are in units of m_W^2.

ξ	$\Delta\sigma^{(1)}_{\rm fin}$	$\Delta\sigma^{(2)}_{\rm fin}$	$\Delta\sigma_{\rm sub}$	$\Delta\sigma_{\rm tot}$	$g^2\sigma_{\rm cl}/\pi$
0.5	0.244	−0.001	−0.731	−0.488	0.757 42
0.6	0.204	0.002	−0.773	−0.567	0.813 06
0.7	0.176	0.005	−0.795	−0.615	0.864 41
0.8	0.154	0.009	−0.811	−0.649	0.912 32
0.9	0.135	0.014	−0.825	−0.675	0.957 37
1.0	0.119	0.022	−0.837	−0.700	1.0000
1.1	0.105	0.030	−0.848	−0.713	1.0405
1.2	0.092	0.041	−0.859	−0.726	1.0792
1.3	0.080	0.054	−0.870	−0.736	1.1163
1.4	0.069	0.069	−0.881	−0.743	1.1518
1.5	0.058	0.086	−0.891	−0.747	1.1860
1.6	0.048	0.107	−0.902	−0.747	1.2190
1.7	0.038	0.130	−0.913	−0.745	1.2509
1.8	0.028	0.155	−0.923	−0.740	1.2818
1.9	0.018	0.184	−0.934	−0.731	1.3116
2.0	0.009	0.216	−0.944	−0.719	1.3406

At large p the subtracted integrand should behave as p^{-6}. For the Faddeev-Popov sector this is realized in ideal form. For the gauge-Higgs sector there are deviations for $p > 6$, which remain even if higher partial waves are included. So they seem to be caused by some very small numerical deficiencies in the low partial waves. Their origin is difficult to localize. As these contributions only appear above $p \simeq 6$, we have done least-square fits of the form $A/p^6 + B/p^8$ based on the data points between $p = 2$ and $p = 6$. These fits then were used in order to append the integrals from $p = 6$ to ∞. The fits are displayed in Figs. 18 and 19 for the gauge-Higgs and Faddeev-Popov sectors, respectively.

The integrals over the subtracted part of the function $F(p)$, including the asymptotic tail based on the fits, are given in Table I; they are denoted as $\Delta\sigma_{\rm sub}$.

Now that we have computed the subtracted integrals, we have to add back the regularized and renormalized divergent contributions. Those with one vertex are given, in unrenormalized form, by

$$\begin{aligned}\Delta\sigma^{(1)} &= \Delta\sigma_{\rm fl,33} + \Delta\sigma_{\rm fl,44} \\ &= -\frac{m_W^2}{32\pi^2}\left\{\left(L_\epsilon + 1 - \ln\frac{m_W^2}{\mu^2}\right)(1+2\xi^2) \right. \\ &\quad \left. -\frac{3}{2}\xi^2\ln\xi^2\right\}\int d^2x(f^2(r)-1), \end{aligned} \tag{7.5}$$

see Eqs. (6.12) and (6.13), as well as the comment below Eq. (6.14). One may choose the renormalization such as to omit these tadpole contributions entirely, as one would do in the 1 + 1 dimensional theory, using normal ordering the field operators. Here we use the strict $\overline{MS}$ scheme and choose the renormalization scale as $\mu^2 = m_W^2$. Therefore, we have to add back

$$\begin{aligned}\Delta\sigma^{(1)}_{\rm fin} &= -\frac{m_W^2}{32\pi^2}\left\{\left(1-\ln\frac{m_W^2}{\mu^2}\right)(1+2\xi^2) - \frac{3}{2}\xi^2\ln\xi^2\right\} \\ &\quad \times \int d^2x(f^2(r)-1). \end{aligned} \tag{7.6}$$

As we separately present this contribution in Table I, the reader may easily change this contribution according to her/his own preferences.

For computing the finite parts of the graphs with two vertices, as given in Eqs. (6.22), (6.25), (6.26), (6.27), (6.31), (3.6), and (6.49), we need the Fourier-Bessel transforms of the classical profiles, as defined in Secs (VI A)–(VI E), and the second-order kernels as defined in Appendix G. The numerical evaluation is straightforward, the Fourier-Bessel transforms were checked using the Parseval equation. The sum of these contributions is denoted as

$$\begin{aligned}\Delta\sigma^{(2)}_{\rm fin} &= \Delta\sigma_{\rm fl,11,11} + \Delta\sigma_{\rm fl,22,22} + \Delta\sigma_{\rm fl,33,33} + \Delta\sigma_{\rm fl,44,44} \\ &\quad + \Delta\sigma_{\rm fl,55,55} + \Delta\sigma_{\rm fl,(12)3,(12)3} + \Delta\sigma_{\rm fl,(12)4,(12)4} \\ &\quad + \Delta\sigma_{\rm fl,34,34}. \end{aligned} \tag{7.7}$$

The separate results for the graphs with one vertex, $\Delta\sigma^{(1)}_{\rm fin}$, for the graphs with two vertices $\Delta\sigma^{(2)}_{\rm fin}$, the subtracted contribution $\Delta\sigma_{\rm sub}$, and the total one-loop contribution $\Delta\sigma_{\rm tot}$ are listed in Table I and displayed in Fig. 20. Table I and Fig. 20 also include the values of the classical string tension. We should like to recall that the subtracted contribution still includes some gauge field graphs with two vertices, which by themselves are divergent, but whose

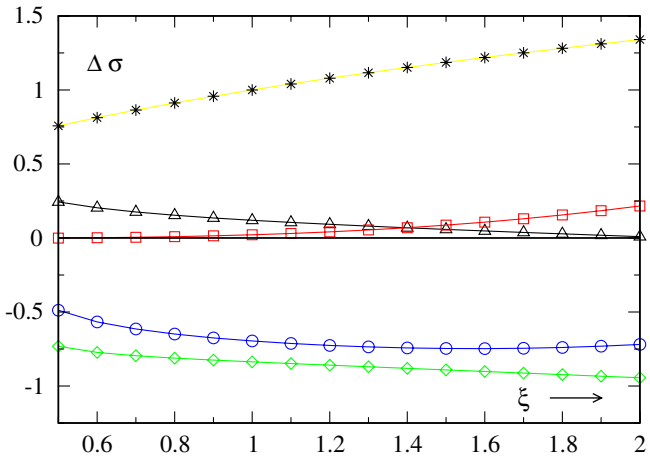

FIG. 20 (color online). The correction to the string tension as a function of $\xi = m_H/m_W$. Squares: contributions with one vertex $\Delta\sigma^{(1)}$; triangles: contributions with two vertices $\Delta\sigma^{(2)}$; diamonds: subtracted contribution $\Delta\sigma_{\rm sub}$; circles: total one-loop correction $\Delta\sigma_{\rm tot}$; asterisks: the classical string tension multiplied by g^2/π. All string tensions are in units of m_W^2.

divergences are canceled by higher order vertex graphs, as discussed in Sec. VI F.

VIII. SUMMARY

We have presented here a numerical computation of the one-loop corrections to the string tension of the Nielsen-Olesen vortex in the $3+1$ dimensional Abelian Higgs model, taking into account the fluctuations of gauge, the Higgs, and the Faddeev-Popov fields. One of the main complications arose from the fact that the divergences of graphs with external gauge field loops require cancellations of Feynman graphs with different numbers of external vertices. This has required an extensive discussion of vertex graphs and vacuum Feynman graphs. On the numerical side, we had to adapt a previously developed computation scheme to this new situation. We had to find and have found a way of implementing the necessary cancellations, which are relatively straightforward when done analytically, into the numerical procedure.

The computation is exact to one-loop order in the sense that the equations on which it is based, Eqs. (5.5), (5.6), (5.7), and (5.13), constitute an exact expression for the unrenormalized one-loop string tension, and that the expressions defining the subtractions and the finite parts to be added back, as given in the various subsections of Sec. VI, constitute an exact framework for the computation of the renormalized one-loop string tension. Of course these analytical expressions have to be evaluated numerically, and of course numerical computations are always of limited accuracy. Some of these, like the accuracy in the low partial waves, can be improved by using still better profiles, using, e.g., finer grids, by a more precise solution of the differential equations, beyond the four-step Runge-Kutta we used here. A problem of a more basic nature is the use of extrapolations both in angular momentum n and in momentum p. The asymptotic behavior of the leading orders in the vertex expansion can be cross-checked, as described in Sec. VII. For the very small subtracted parts the asymptotic power behavior in n is expected to set in only if n is much larger as pR, where R is a typical radius of the classical solution, and vice versa for the asymptotic behavior in p. The fact that using our power fit summation in n leads finally to a p^{-6} of $F_{\mathrm{sub}}(p)$ behavior represents a valuable and—in our opinion—satisfactory cross-check. However, we are faced here with a subtraction which, already at $p=10$, reduces the unsubtracted integrand by 4 orders of magnitude. So even very small errors, e.g., in the low partial waves, will set limits to an "ultimate" verification of this power behavior at really large p. The use of uniform expansions of Bessel functions as proposed in Ref. [38] could be helpful, but its application to a coupled system and to the twice subtracted integrand would constitute, to the least, a very involved research project.

The size of the corrections of course depends on the renormalization scheme and renormalization conditions. We here have adapted the $\overline{MS}$ scheme with m_W^2 as the renormalization scale. The corrections are sizable, but small with respect to the classical string tension as long as the gauge coupling g is smaller than unity, which may be considered as a reasonable assumption. Unlike in the case of the fermionic corrections, we do not have at our disposal an extra parameter, the Yukawa coupling, that could render the corrections important for heavy fermions. The parameters are fixed already at the classical level.

Of course, in the present situation of cosmic string phenomenology a precise information on the string tensions and corrections to it cannot be considered as very important. Indeed we consider as our main result that we presented a method for computing such corrections in a gauge theory with all its technical complications. The situation may be different if these corrections are computed at finite temperature, as it may be realistic in primordial cosmology. Such computations, using similar techniques, have been done for bubble nucleation in Ref. [39]. In the high-temperature approximation to the electroweak theory, the corrections to the transition rate were found to be huge [40,41].

A further application of the methods presented here may be the investigation of the role of quantum fluctuations for the electroweak string, in particular, in the context of its stabilization [42]

APPENDIX A: PARTIAL WAVE DECOMPOSITION OF THE FREE GREEN'S FUNCTION

We shortly recall the partial wave decomposition of the free Green's function, a decomposition that is used repeatedly in the subtraction procedure. We here consider the Green's function in two dimensions, with an effective mass $\kappa^2 = m^2 + p^2$; the one in four dimensions is obtained by replacing $p^2 = \nu^2 + k_3^2$ and by further integrations over ν and k_3. We further omit the subscript $\perp$, replacing $\mathbf{x}_\perp \to \mathbf{x}$ and $\mathbf{k}_\perp \to \mathbf{k}$. The free Green's function $G_0(\mathbf{x}, \mathbf{x}', \kappa)$ is defined as

$$G_0(\mathbf{x}, \mathbf{x}', \kappa) = \int \frac{d^2k}{(2\pi)^2} \frac{e^{i\mathbf{k}\cdot(\mathbf{x}-\mathbf{x}')}}{\mathbf{k}^2 + \kappa^2}. \tag{A1}$$

It can be computed readily, using formulas (9.1.18) and (11.4.44) of Ref. [43]:

$$\begin{aligned} G_0(\mathbf{x}, \mathbf{x}', \nu) &= \frac{1}{4\pi^2} \int_0^\infty k dk \int_0^\pi d\phi \frac{2\cos(kR\cos\phi)}{k^2 + \kappa^2} \\ &= \frac{1}{2\pi} \int_0^\infty \frac{dk k J_0(kR)}{k^2 + \kappa^2} = \frac{1}{2\pi} K_0(\kappa R), \end{aligned} \tag{A2}$$

with $R = |\mathbf{x} - \mathbf{x}'|$. Furthermore this may be expanded, using Eq. (4) in section 7.6.1 of Ref. [44] as

$$G_0(\mathbf{x}, \mathbf{x}', \nu) = \frac{1}{2\pi} \sum_{k=-\infty}^{\infty} K_n(\kappa r_>) I_n(\kappa r_<) e^{in\phi}. \quad \text{(A3)}$$

APPENDIX B: FIRST-ORDER CONTRIBUTIONS TO THE PARTIAL WAVES

Using the formula for the free Green's function derived in Appendix A the first-order contribution to the Green's function in two dimensions is given by

$$\begin{aligned} G^{(1)}(\mathbf{x}, \mathbf{x}', p) &= -\int d^2x'' G_0(\mathbf{x}, \mathbf{x}'', \kappa) V(r'') G_0(\mathbf{x}'', \mathbf{x}', \kappa) \\ &= -\frac{1}{4\pi^2} \int dr'' r'' d\phi'' \sum_{n=-\infty}^{\infty} \sum_{n'=-\infty}^{\infty} K_n(\kappa r_>) I_n(\kappa r_<) e^{in(\phi-\phi'')} V(r'') K_{n'}(\kappa r'_>) I_{n'}(\kappa r'_<) e^{in'(\phi''-\phi')} \\ &= -\frac{1}{2\pi} \int dr'' r'' \sum_{n=-\infty}^{\infty} K_n(\kappa r_>) I_n(\kappa r_<) e^{in(\phi-\phi')} V(r'') K_n(\kappa r'_>) I_n(\kappa r'_<), \end{aligned} \quad \text{(B1)}$$

where $r_> = \max\{r, r''\}$, $r'_> = \max\{r', r''\}$, and similarly for $r_<$ and $r'_<$. The "potential" $V(r)$ subsumes all vertex contributions appearing in first order.

We define

$$G^{(1)}(\mathbf{x}, \mathbf{x}', p) = \frac{1}{2\pi} \sum_{n=-\infty}^{\infty} e^{in(\phi-\phi')} G_n^{(1)}(r, r', p) \quad \text{(B2)}$$

and therefore get

$$G_n^{(1)}(r, r, p) = -\int dr'' r'' K_n^2(\kappa r_>) I_n^2(\kappa r_<) V(r''). \quad \text{(B3)}$$

Using the integrals of Appendix D, this can be integrated over rdr with the result

$$\begin{aligned} \int_0^\infty dr r G_n^{(1)}(r, r, p) = -\int_0^\infty dr' r' V(r') \frac{z}{2\kappa^2} &\times \{-2n[I_{n+1}(z) I_n(z) K_n^2(z) \\ &+ K_{n+1}(z) K_n(z) I_n^2(z)] \\ &+ z[K_{n+1}^2(z) I_n^2(z) \\ &- I_{n+1}^2(z) K_n^2(z)]\}, \end{aligned} \quad \text{(B4)}$$

with $z = \kappa r'$. Using the Wronskian relation

$$I_n(z) K_{n+1}(z) + I_{n+1}(z) K_n(z) = \frac{1}{z}, \quad \text{(B5)}$$

this can be rewritten as

$$\begin{aligned} \int_0^\infty dr r G_n^{(1)}(r, r, p) &= -\int_0^\infty dr' r' V(r') \frac{1}{2\kappa^2} \\ &\times \{-2n I_n(z) K_n(z) \\ &+ z[K_{n+1}(z) I_n(z) - I_{n+1}(z) K_n(z)]\} \\ &= -\int_0^\infty dr' r' V(r') \frac{1}{2\kappa} \frac{d}{d\kappa} I_n(z) K_n(z). \end{aligned} \quad \text{(B6)}$$

This is the contribution of one partial wave to the sum over partial waves, which is then to be integrated with respect to ν and k_3 to yield the string tension in first order. However, the sum over partial waves and the integrals are divergent; the perturbative contribution has to be subtracted from the full, nonperturbative contribution of each partial wave in order to obtain convergent summations and integrations. We may check that formally the first-order perturbative contributions can be summed up and integrated so as to reobtain the Feynman integral. The sum over partial waves of this expression yields

$$\begin{aligned} &-\sum_{n=-\infty}^{\infty} \frac{1}{p} \frac{d}{dp} \int_0^\infty dr' r' V(r') I_n(z) K_n(z) \\ &= -2\pi \frac{1}{2p} \frac{d}{dp} \int_0^\infty dr' r' V(r') G_0(\mathbf{x}, \mathbf{x}, \kappa) \\ &= -\frac{1}{2p} \frac{d}{dp} \int d^2x V(|\mathbf{x}|) \int \frac{d^2k_\perp}{(2\pi)^2} \frac{1}{\mathbf{k}_\perp^2 + m^2 + p^2}. \end{aligned} \quad \text{(B7)}$$

Going back to Sec. V we see that we have to integrate this with $-\int p^3 dp/4\pi$. We obtain

$$\begin{aligned} \sigma^{(1)} &= -\frac{1}{2} \int d^2x V(|\mathbf{x}|) \int \frac{p^3 dp d^2k_\perp}{(2\pi)^3} \frac{1}{2p} \frac{d}{d\nu} \\ &\quad \times \frac{1}{\mathbf{k}_\perp^2 + p^2 + m^2} \\ &= -\frac{1}{2} \int d^2x V(|\mathbf{x}|) \int \frac{p dp d^2k_\perp}{(2\pi)^3} \frac{1}{\mathbf{k}_\perp^2 + p^2 + m^2} \\ &= -\frac{1}{2} \int d^2x V(|\mathbf{x}|) \int \frac{d\nu d^3k}{(2\pi)^4} \frac{1}{\mathbf{k}^2 + \nu^2 + m^2}, \end{aligned} \quad \text{(B8)}$$

where in the last step we have substituted $p^2 = k_3^2 + \nu^2$. The result is indeed the first-order vacuum graph.

APPENDIX C: SECOND-ORDER CONTRIBUTION TO THE PARTIAL WAVES

Using similar steps as in Appendix B and using again the integrals in Appendix D and Wronskian relations, we find that the second-order contribution to the partial waves is given by

$$\int drrG_n^{(2)}(r,r,p) = \sum_{ij}\int dr'r'V_{ij}^n(r')\int dr''r''V_{ji}^n(r'') \times I_{n_i}(\kappa_i r_<)K_{n_i}(\kappa_i r_>)\left(-\frac{1}{2\kappa_j}\frac{d}{d\kappa_j}\right) \times I_{n_j}(\kappa_j r_<)K_{n_j}(\kappa_j r_>), \tag{C1}$$

where $r_< = \min(r', r'')$ and $r_> = \max(r', r'')$. The computation is quite lengthy, as we start with an expression where the values r, r', and r'' appear in six different orderings. Here we have written all relevant indices, as the two propagators have, in general, different masses and angular momenta. We note that the differentiation with respect to $\kappa_j = \sqrt{p^2 + m_j^2}$ can be written as a differentiation with respect to p if the combinations $V_{ij}V_{ji}$ and $V_{ji}V_{ij}$ are combined. If applied to the sum over i and j, this results in a double counting that has to be compensated by a factor $1/2$. So

$$\int drrG_n^{(2)}(r,r,p) = \frac{1}{2}\left(-\frac{1}{2p}\frac{d}{dp}\right)\sum_{ij}\int dr'r'V_{ij}^n(r') \times \int dr''r''V_{ji}^n(r'')I_{n_i}(\kappa_i r_<) \times K_{n_i}(\kappa_i r_>)I_{n_j}(\kappa_j r_<)K_{n_j}(\kappa_j r_>). \tag{C2}$$

APPENDIX D: SOME INTEGRALS

In our calculations we repeatedly need some integrals over Bessel functions which we write down here, without derivation. They can be obtained from Eq. (11.3.29) of Ref. [43] by taking the limit $k \to l$ (see there). The formulas are

$$\int_0^r drrI_n^2(\kappa r) = \frac{z}{2\kappa^2}\{-2nI_{n+1}(z)I_n(z) + z[I_n^2(z) - I_{n+1}^2(z)]\}, \tag{D1}$$

$$\int_r^\infty drrK_n^2(\kappa r) = \frac{z}{2\kappa^2}\{-2nK_{n+1}(z)K_n(z) - z[K_n^2(z) - K_{n+1}^2(z)]\}, \tag{D2}$$

$$\int^r drrI_n(\kappa r)K_n(\kappa r) = \frac{z}{2\kappa^2}\{n[K_{n+1}(z)I_n(z) - K_n(z)I_{n+1}(z)] + z[I_n(z)K_n(z) + I_{n+1}(z)K_{n+1}(z)]\}, \tag{D3}$$

with $z = \kappa r$. Note the limits of integration; the third integral is an indefinite one.

APPENDIX E: SOME USEFUL SUMS

We define the two-dimensional Green's function $G_2^{(0)}(\mathbf{x}, \mathbf{x}', \nu^2)$ as the solution of the equation

$$[-\Delta_2 + m^2 + \nu^2]G_{(0)}^2 = \delta^2(\mathbf{x} - \mathbf{x}'). \tag{E1}$$

We readily obtain

$$G_2^{(0)}(\mathbf{x}, \mathbf{x}', \nu^2) = \int \frac{d^2k}{(2\pi)^2}\frac{e^{i\mathbf{k}(\mathbf{x}-\mathbf{x}')}}{\mathbf{k}^2 + m^2 + \nu^2}. \tag{E2}$$

The integral may be done explicitly with the result

$$G_2^{(0)}(\mathbf{x}, \mathbf{x}', \nu^2) = \frac{1}{2\pi}K_0(\kappa R), \tag{E3}$$

with

$$R = |\mathbf{x} - \mathbf{x}'| = \sqrt{r^2 + r'^2 - 2rr'\cos(\varphi - \varphi')}. \tag{E4}$$

Furthermore the Gegenbauer expansion of the modified Bessel function yields

$$G_2^{(0)}(\mathbf{x}, \mathbf{x}', \nu^2) = \frac{1}{2\pi}\sum_{n=-\infty}^{\infty} e^{in(\varphi-\varphi')}I_n(\kappa r_<)K_n(\kappa r_>). \tag{E5}$$

The limit $\mathbf{x} \to \mathbf{x}'$ of the Green's function does not exist. However, what we need is

$$-\frac{1}{2\kappa}\frac{d}{d\kappa}\sum_{n=-\infty}^{\infty} I_n(\kappa r)K_n(\kappa r). \tag{E6}$$

We note that

$$-\frac{1}{2\kappa}\frac{d}{d\kappa}K_0(\kappa R) = \frac{R}{2\kappa}K_1(\kappa R). \tag{E7}$$

The limit $R \to 0$ exists and one obtains

$$-\frac{1}{2\kappa}\frac{d}{d\kappa}\sum_{n=-\infty}^{\infty} I_n(\kappa r)K_n(\kappa r) = \frac{1}{2\kappa^2}. \tag{E8}$$

APPENDIX F: FOURIER-BESSEL TRANSFORMS

For the evaluation of the perturbative contributions, we need the Fourier transform of the external sources. Let us consider at first a scalar field $\Phi(r_\perp)$, independent of Euclidean time τ and z. In our application ϕ will be $f(r_\perp) - 1$, $f^2(r_\perp) - 1$ etc. We have

$$\tilde{\Phi}(q_0, q_z, q_\perp) = \int d^4x e^{-ip\cdot x}\Phi(r_\perp) = (2\pi)^2\delta(p_0)\delta(p_z)\int_0^\infty dr r \times \int_{-\pi}^{\pi} d\varphi \Phi(r) e^{-iq_\perp r\cos\varphi} \quad \text{(F1)}$$

$$= (2\pi)^3\delta(p_0)\delta(p_z) \times \int_0^\infty r dr \Phi(r) J_0(q_\perp r). \quad \text{(F2)}$$

In the following we will omit the trivial factor $(2\pi)^2\delta(p_0)\delta(p_z)$ originating from the τ and z integrations and write

$$\tilde{\Phi}(q) = \chi_\Phi(q) = 2\pi\int_0^\infty r dr \Phi(r) J_0(qr) \quad \text{(F3)}$$

implying $q \sim q_\perp$. The relation between the Fourier-Bessel transformation and the inverse transformation implies the relation

$$\int q dq J_l(qr) J_l(qr') = \frac{1}{r}\delta(r - r') \quad \text{(F4)}$$

for arbitrary l. We deduce the Parseval equation

$$\int \frac{d^2q}{(2\pi)^2}|\chi_\Phi(q)|^2 = \int \frac{dqq}{2\pi}|\chi_\Phi(q)|^2 = 2\pi\int_0^\infty r dr |\Phi(r)|^2 = \int d^2x |\Phi(r)|^2, \quad \text{(F5)}$$

which can be used as a numerical cross-check. If one disregards $V_{34} = V_{43}$ and the gauge field parts of V_{33} and V_{44}, these Fourier-Bessel transforms are unproblematic. We shortly discuss the various components.

In the diagonal we have the Higgs field parts which are proportional to $f^2(r) - 1$. This function goes to zero exponentially as $r \to \infty$, so the Fourier transform exists. It is found to decrease exponentially at large q.

Considering the contribution of $V_{13} = V_{23} = \sqrt{2}m_W f'$, the function $f'(r)$ decays exponentially as $r \to \infty$ and goes to a constant as $r \to 0$. So $\tilde{V}_{13}(q)$ exists. It is found to decrease as $1/q^2$.

The function $V_{14}(r) = \sqrt{2}m_W f(A + 1)/r$ goes to a constant as $r \to 0$ and decreases exponentially as $r \to \infty$. So again the Fourier transform exists, and again it decreases as $1/q^2$.

All the Fourier transforms discussed up to now have to be folded with the Feynman integral kernels (see Appendix G) which behave as $\ln q^2$ at large q. One easily convinces oneself that the integrals over the kernels times the squared Fourier transforms are well convergent.

The Fourier transform of the gauge field

$$A_i^\perp = \epsilon_{ij}\hat{x}_j\frac{A(r) + 1}{r} \quad \text{(F6)}$$

is problematic. The function is not square integrable; due to the singularity at $r = 0$ its norm diverges logarithmically. So the Fourier transform is not square integrable either. Nevertheless it can be computed. The Fourier transform must be of the form

$$\tilde{A}_i^\perp(q) = \epsilon_{ij}\hat{q}_j\chi_A(q). \quad \text{(F7)}$$

We have

$$\chi_A(q) = \epsilon_{ij}\hat{q}_j\tilde{A}_i^\perp(q) = \epsilon_{ij}\epsilon_{ik}\int d^2x \frac{A(r) + 1}{r} e^{-i\vec{q}\,\vec{r}}\hat{q}_j\hat{x}_k = \int_0^\infty r dr \frac{A(r) + 1}{r}\int_{-\pi}^{\pi} e^{-iqr\cos\varphi}\cos\varphi = 2\pi\int_0^\infty r dr \frac{A(r) + 1}{r} J_1(qr). \quad \text{(F8)}$$

The function $\chi_A(q)$ behaves as βq as $q \to 0$ with

$$\beta = \pi\int_0^\infty r dr (A(r) + 1), \quad \text{(F9)}$$

and like $2\pi/q$ as $r \to \infty$. This asymptotic behavior makes the square norm of the Fourier transform logarithmically divergent, as a reflection of the logarithmic divergence of the norm of the field $A_i^\perp(r)$. The handling of the graphs with two external gauge field legs is discussed in some detail is Sec. VI E.

APPENDIX G: THE SECOND-ORDER KERNELS

The finite parts of the second-order graphs all contain an integral

$$\mathcal{I}(m_a^2, m_b^2, q^2) = \int_0^1 d\omega \log[\omega(1 - \omega)q^2 + \omega m_a^2 + (1 - \omega)m_b^2]. \quad \text{(G1)}$$

We generally assume $m_a^2 > 0, m_b^2 > 0$. If furthermore $q^2 > 0$ then we define

$$\omega_\pm = \frac{1 + m_a^2 - m_b^2}{2q^2} \pm \sqrt{\frac{(1 + m_a^2 - m_b^2)^2 + 4m_b^2q^2}{4q^4}}. \quad \text{(G2)}$$

One easily realizes that $\omega_+ > 1$ and $\omega_- < 0$. With this definition $\mathcal{I}$ is given by

$$\mathcal{I}(ma^2, m_b^2, q^2) = \omega_+\ln\omega_+ + \omega_-\ln(-\omega_-) + (1 - \omega_+)\ln(\omega_+ - 1) + (1 - \omega_-) \times \ln(1 - \omega_-) + \ln q^2 - 2. \quad \text{(G3)}$$

This expression is symmetric in m_a^2 and m_b^2.

If $q^2 = 0$ the integral is given, for $m_a^2 \neq m_b^2$, by

$$\mathcal{I}(m_a^2, m_b^2, 0) = \frac{m_a^2 \ln m_a^2 - m_b^2 \ln m_b^2}{m_a^2 - m_b^2} - 1. \tag{G4}$$

Finally, if $m_a^2 = m_b^2$ we have

$$\mathcal{I}(m_a^2, m_a^2, 0) = \ln m_a^2. \tag{G5}$$

For small q^2 the integral behaves as $c_1 + c_2 q^2$, where the constant c_1 is of course identical to $\mathcal{I}^2(m_a^2, m_b^2, 0)$. For large q^2 the integral behaves as $\ln q^2 + \text{const} + O(1/q^2)$.

The correction to the gauge boson propagator, the term $\Delta\sigma_{\text{fl},3434}$ contains an integral

$$\mathcal{J} = \int_0^1 d\omega \mathcal{Q}^2 \left[\ln \frac{\mathcal{Q}^2}{\mu^2} - 1 \right], \tag{G6}$$

with $\mathcal{Q}^2 = \omega m_H^2 + (1-\omega) m_W^2 + \omega(1-\omega)\mathbf{q}^2$. Using the same conventions for ω_- and ω_+ with $m_a = m_w$, $m_b = m_H$. It is given by

$$\mathcal{J} = q^2[(9\omega_- + 9\omega_+ - 18\omega_-\omega_+ - 6)\ln(-\omega_-\omega_+ + \omega_- + \omega_+ - 1) + (9\omega_- + 9\omega_+ - 18\omega_-\omega_+ - 6)\ln q^2 + 3\omega_-^2(3\omega_+ - \omega_-)\ln\frac{1-\omega_-}{-\omega_-} + 3\omega_+^2(3\omega_- - \omega_+)\ln\frac{\omega_+ - 1}{\omega_+} - 3\omega_-^2 + 18\omega_-\omega_+ - 6\omega_- - 3\omega_+^2 - 6\omega_+ + 4]/18. \tag{G7}$$

[1] A. Achucarro and T. Vachaspati, Phys. Rep. **327**, 347 (2000).
[2] F. A. Schaposnik, arXiv:hep-th/0611028.
[3] T. W. B. Kibble, J. Phys. A **9**, 1387 (1976).
[4] A. Vilenkin, Phys. Rep. **121**, 263 (1985).
[5] M. B. Hindmarsh and T. W. B. Kibble, Rep. Prog. Phys. **58**, 477 (1995).
[6] A. Vilenkin, arXiv:hep-th/0508135.
[7] M. Sakellariadou, Lect. Notes Phys. **718**, 247 (2007).
[8] A. A. Abrikosov, Sov. Phys. JETP **32**, 1442 (1957).
[9] H. B. Nielsen and P. Olesen, Nucl. Phys. **B61**, 45 (1973).
[10] M. Bordag and I. Drozdov, Phys. Rev. D **68**, 065026 (2003).
[11] M. Groves and W. B. Perkins, Nucl. Phys. **B573**, 449 (2000).
[12] M. Bordag, Phys. Rev. D **67**, 065001 (2003).
[13] D. V. Vassilevich, Phys. Rev. D **68**, 045005 (2003).
[14] N. Graham, V. Khemani, M. Quandt, O. Schroeder, and H. Weigel, Nucl. Phys. **B707**, 233 (2005).
[15] M. Goodband and M. Hindmarsh, Phys. Lett. B **363**, 58 (1995).
[16] A. Alonso Izquierdo *et al.*, arXiv:hep-th/0611180.
[17] A. A. Izquierdo, W. Garcia Fuertes, M. de la Torre Mayado, and J. Mateos Guilarte, J. Phys. A **39**, 6463 (2006).
[18] J. Baacke, Z. Phys. C **47**, 263 (1990).
[19] J. Baacke, Z. Phys. C **47**, 619 (1990).
[20] J. Baacke, Z. Phys. C **53**, 402 (1992).
[21] J. Baacke, Acta Phys. Pol. B **22**, 127 (1991).
[22] *Potential Scattering*, edited by V. de Alfaro and T. Regge (North-Holland, Amsterdam, 1965).
[23] M. Bordag and K. Kirsten, Phys. Rev. D **53**, 5753 (1996).
[24] N. Graham *et al.*, Nucl. Phys. **B645**, 49 (2002).
[25] N. Graham, R. L. Jaffe, and H. Weigel, Int. J. Mod. Phys. A **17**, 846 (2002).
[26] N. Graham *et al.*, Phys. Lett. B **572**, 196 (2003).
[27] J. Baacke and N. Kevlishvili, Phys. Rev. D **71**, 025008 (2005).
[28] J. Baacke and N. Kevlishvili, Phys. Rev. D **75**, 045001 (2007).
[29] J. Baacke and H. Sprenger, Phys. Rev. D **60**, 054017 (1999).
[30] H. J. de Vega and F. A. Schaposnik, Phys. Rev. D **14**, 1100 (1976).
[31] F. A. Schaposnik, Phys. Rev. D **18**, 1183 (1978).
[32] We use Euclidean notation for the transverse components, so $A_1^\perp \equiv A^1 = -A_1$ etc.
[33] J. Baacke and T. Daiber, Phys. Rev. D **51**, 795 (1995).
[34] J. Baacke, arXiv:0803.4333 [Phys. Rev. D (to be published)].
[35] F. A. Bais and J. R. Primack, Phys. Rev. D **13**, 819 (1976).
[36] J. Kripfganz and A. Ringwald, Mod. Phys. Lett. A **5**, 675 (1990).
[37] J. Baacke and A. Surig, Z. Phys. C **73**, 369 (1997).
[38] G. V. Dunne, J. Hur, and C. Lee, Phys. Rev. D **74**, 085025 (2006).
[39] J. Baacke and V. G. Kiselev, Phys. Rev. D **48**, 5648 (1993).
[40] J. Kripfganz, A. Laser, and M. G. Schmidt, Nucl. Phys. **B433**, 467 (1995).
[41] J. Baacke, Phys. Rev. D **52**, 6760 (1995).
[42] M. Nagasawa and R. Brandenberger, Phys. Rev. D **67**, 043504 (2003).
[43] *Handbook of Mathematical Functions*, edited by I. Abramowitz and M. Stegun (Dover Publications, New York, 1968).
[44] *Higher Transcendental Functions*, edited by A. Erdelyi (McGraw-Hill Book Company, Inc., New York, 1953).